

Designing biocatalytic redox reactions with oxidoreductases for organic chemistry

Rauch, Marine

DOI

[10.4233/uuid:afcbf229-f6ba-4b81-a561-6a0a61dc74de](https://doi.org/10.4233/uuid:afcbf229-f6ba-4b81-a561-6a0a61dc74de)

Publication date

2020

Document Version

Final published version

Citation (APA)

Rauch, M. (2020). *Designing biocatalytic redox reactions with oxidoreductases for organic chemistry*. [Dissertation (TU Delft), Delft University of Technology]. <https://doi.org/10.4233/uuid:afcbf229-f6ba-4b81-a561-6a0a61dc74de>

Important note

To cite this publication, please use the final published version (if applicable). Please check the document version above.

Copyright

Other than for strictly personal use, it is not permitted to download, forward or distribute the text or part of it, without the consent of the author(s) and/or copyright holder(s), unless the work is under an open content license such as Creative Commons.

Takedown policy

Please contact us and provide details if you believe this document breaches copyrights. We will remove access to the work immediately and investigate your claim.

Designing biocatalytic redox reactions with oxidoreductases for organic chemistry

Dissertation

for the purpose of obtaining the degree of doctor

at Delft University of Technology

by the authority of the Rector Magnificus, Prof.dr.ir. T.H.J.J. van der Hagen,

chair of the Board for Doctorates

to be defended publicly on

Friday 27th of March 2020 at 10:00 o'clock

By

Marine Charlène Renée RAUCH

Ingénieure diplômée de l'Ecole Nationale Supérieure de Chimie de Mulhouse,
Université de Haute Alsace, France

Born in Sarreguemines, France

This dissertation has been approved by the promotor.

Composition of the doctoral committee:

Rector Magnificus,	chairperson
Prof. dr. F. Hollmann	Delft University of Technology, promotor
Prof. dr. I.W.C.E. Arends	Utrecht University, promotor
Dr. C.E. Paul	Delft University of Technology, copromotor

Independent members:

Prof. Dr. U. Hanefeld	Delft University of Technology
Prof. dr. D. Holtmann	TH Mittelhessen, Germany
Prof. dr. T. Tron	Université de Aix-Marseille, France
Dr. R. Zuhse	Chiracon GmbH, Germany
Prof. dr. P. Daran-Lapujade	Delft University of Technology, reserve member

The research reported in this thesis was supported by the European Research Council (ERC Consolidator Grant No. 648026).

Printed by: Gildeprint, Enschede
Cover by: Delphine Rauch and Anne Gerbig
ISBN/EAN: 978-94-6384-112-2

Table of contents

Summary and Nederlandse samenvatting	7
Chapter 1: Introduction	17
Chapter 2: Photobiocatalytic alcohol oxidation using LED light source	41
Chapter 3: Photochemical regeneration of flavoenzymes – an Old Yellow Enzyme case study	59
Chapter 4: Metals in biotechnology: Cr-driven-stereoselective reduction of conjugated C=C-double bonds	79
Chapter 5: Peroxygenase-catalysed epoxidation of styrene derivatives in neat reaction media	91
Chapter 6: Conclusions and recommendations	107
Curriculum vitae and list of publications	117
Acknowledgements	123

**Summary
and
Nederlandse samenvatting**

Summary

The focus of this thesis is to identify improvements of oxidoreductase reactions to bring them to preparative scale. Three approaches were studied: (1) photoregeneration of oxidised nicotinamide cofactors with LEDs as light source and flavins, (2) direct regeneration of Old Yellow Enzymes with light or metals, (3) heme-thiolate enzyme peroxygenases in neat substrate conditions.

Flavins are the main actors of the first two approaches. These redox cofactors have been chosen for their photocatalytic properties as a photosensitiser and as a cofactor in the so-called flavoproteins.

Photoexcited flavins are reduced in the presence of electrons donors. This principle was applied for the regeneration of NAD(P)^+ through the use of a flavin and NAD(P)H (**Chapter 2**). A cheap light source, LED, was chosen to promote this approach. Generated NAD^+ was consumed by horse liver alcohol dehydrogenase (HLADH) to achieve the lactonisation of α,ω -diols such as *meso*-3-methyl-1,5-pentanediol. Due to acidification of the reaction at higher substrate loading, process improvements are necessary for up-scale.

In **Chapter 3**, we attempt to up-scale the direct photoregeneration of Old Yellow Enzymes, especially YqjM from *Bacillus subtilis* with LEDs. Photoexcited flavins reduced by the presence of ethylenediaminetetraacetic acid (EDTA) are transferring electrons to the enzyme. The impact of light on the system was described and highlights a degradation of both the flavin and the enzyme. These results limit its application for industrial scale.

In **Chapter 4**, an oxygen- and light-free system was explored. This novel approach for regenerating Old Yellow Enzymes is performed with metals, like zinc and chromium powder. The activity of the flavoproteins is stable which allows a longer reaction time. However, issues were identified, such as the need for a high excess of metals. Nevertheless, by using cell-free extracts, only the targeted enzyme was regenerated and therefore no side-products were detected.

Chapter 5 digresses from the rest of the thesis through the use of another type of enzyme: peroxygenases. Epoxidation reactions in neat substrate conditions of styrene derivatives were performed with the Unspecific peroxygenase (UPO). This enzyme achieved high turnover number (TON) in presence of organic peroxide ($t\text{BuOOH}$). The obtained epoxide further underwent chemical ring opening to produce (pseudo)ephedrine.

The results of this thesis provide important knowledge for bringing biocatalytic reactions to preparative scale. Challenges and achievements have been mentioned and will facilitate future research and application in industrial biocatalytic processes.

Nederlandse samenvatting

Dit proefschrift richt zich op het verbeteren van oxidoreductase-reacties met het doel ze geschikt te maken voor gebruik op preparatieve schaal. Deze probleemstelling werd op drie verschillende manieren benaderd: (1) Door middel van fotoregeneratie van geoxideerde cofactoren met behulp van flavines en LED licht, (2) Door middel van directe regeneratie van “Old Yellow Enzymes” met behulp van licht en metalen. (3) het gebruik van peroxygenases, heem-thiolaat enzymen, onder pure substraat-condities.

Flavines spelen de hoofdrol in de eerste twee methodes. Deze redox cofactoren zijn gekozen vanwege hun foto-katalytische eigenschappen als foto-sensibilisator en als cofactor in de zogenaamde flavine-eiwitten.

Foto-geëxciteerde flavines kunnen worden gereduceerd doormiddel van oxidatie van elektron donoren. Dit principe werd toegepast voor de regeneratie van NAD(P)^+ door het gebruik van een flavine en NAD(P)H (**Hoofdstuk 2**). LED licht werd hier gebruikt als goedkope lichtbron. Het gevormde NAD^+ werd vervolgens geconsumeerd door een alcohol dehydrogenase (van paardenlever), om de lactonisatie van α,ω -diolen, zoals *meso*-3-methyl-1,5-pentaandiol te katalyseren. Door de verzuring van het reactiemengsel bij hogere substraat concentraties zijn proces verbeteringen nodig voor verdere opschaling.

In **hoofdstuk 3** word het onderzoek beschreven naar het opschalen van directe fotoregeneratie van “Old Yellow Enzyme”, in het bijzonder de YqjM van *Bacillus subtilis*, met behulp van LED licht. Hierbij werden de foto-geëxciteerde flavines gereduceerd door ethyleendiaminetetraazijnzuur (EDTA), waarna ze de elektronen doorgaven aan het enzym. Vooral de invloed van licht was belangrijk, aangezien dit de degradatie van zowel de flavine als het enzym veroorzaakte. Dit maakt industriële applicatie vooralsnog onmogelijk.

In **hoofdstuk 4** bestudeerden we een systeem zonder zuurstof of licht. Hier werden namelijk metalen, zoals zink en chroom poeder, gebruikt voor de regeneratie van “Old Yellow Enzyme”. De activiteit van de flavine-eiwitten bleef

stabiel in de tijd. Een probleem was echter de behoefte aan grote hoeveelheden metaal in de reactie. Ondanks het gebruik van cel-vrij extract, werd enkel het beoogde enzym geregenereerd waardoor er geen bijproducten aangetoond werden.

Hoofdstuk 5 wijkt af van de overige hoofdstukken in het gebruik van een ander soort enzym: de peroxygenases. Epoxidatie reacties werden uitgevoerd onder pure substraat condities op verschillende styreen-derivaten met behulp van een specifiek peroxygenase (UPO). Dit enzym resulteerde in hoge omzettingen met een organisch peroxide ($t\text{BuOOH}$). De verkregen epoxide onderging verdere ring-opening om zo (pseudo)efedrine te produceren.

De behaalde resultaten in dit proefschrift leveren belangrijke kennis voor het preparatief opschalen van biokatalytische reacties. De uitdagingen en resultaten zijn beschreven en zullen toekomstig onderzoek en toepassingen in de industriële biokatalyse faciliteren.

À ma famille...

Chapter 1:

Introduction

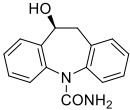
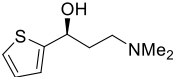
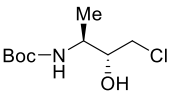
This chapter is based on

G.T. Höfler, F. Hollmann, C.E. Paul, M.C.R. Rauch, M.M.C.H. van Schie, S.J.-P. Willot,
Book chapter submitted.

During the past decades, biocatalysis has gained popularity amongst synthetic organic chemists. The reason is that more isolated enzymes have become available and are powerful catalysts for organic synthesis. Key advantages are the high selectivity of enzyme-catalysed reactions and the mild reaction conditions they operate under. These advantages are valued on lab as well as on industrial scale.¹⁻⁴ Among the diverse classes of enzymes², oxidoreductases occupy a special position. They can replace notoriously demanding reduction and oxidation reactions. In many of these reactions, selectivity and the choice of (stoichiometric) reducing or oxidation reagents are key issues. Oxidoreductases have the potential to improve many of these reactions. They also catalyse an enormous wide range of reactions, from double bond reduction to lactonisation. There is therefore an ongoing and still increasing interest from industry as evidenced by the increasing patent applications dealing with oxidoreductases for large scale organic synthesis.⁵

Overall progress in the engineering of enzymes, in terms of production, immobilisation and structure based stabilisation, has increased the number of industrial enzyme applications worldwide. When scaling up, the main challenge is the stability (and thus maintaining high activity) of the enzyme under industrially desirable conditions. Industrial processes commonly involve high substrate loading and the use of organic solvents. That is because workups and purifications are much more costly and tedious for dilute substrate conditions. The use of organic solvents is favourable because they can be easily removed via distillation, compared to water. These conditions significantly differ from the natural conditions under which enzymes operate. In the case of oxidoreductases, their dependency on cofactors makes upscaling more complex. In parallel to the reaction to be studied, the cofactor needs to be regenerated with high activity and atom efficiency. Numerous examples show great achievements in enzymatic up scaled reactions.⁵ Table 1.1 shows some examples of patented enzymatic synthesis using ketoreductases which dealt with these challenges.

Table 1.1. Patented enzymatic reactions using ketoreductases enabling high product concentration and purity.

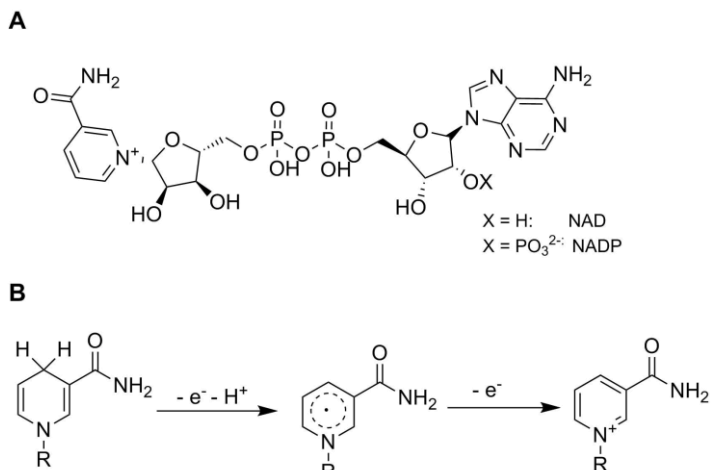
Product generated in the patented enzymatic reaction	Comments	Challenge encountered in the enzymatic reactions	Challenge overcome	Patent owner (reference)
	Reaction highly concentrated: initial substrate loading of 400 g/L	Poor substrate load	Yes	Codexis (6)
	Presence of high concentration of organic solvent: reaction done in 60% isopropanol	Poor stability toward organic solvent	Yes	Codexis (7)
	Effective NADP regeneration using very low concentration of NADP (0.05 g/L)	Dependence on cofactors	Yes	Enzymeworks (8)
	Need of improvements for the crystallisation: only 55% isolated yield	Difficult workups and purification	No, still need improvements for reaching higher isolated yield	Pfizer (9)

Codexis patented an enzymatic reduction of a hindered ketone that is unreactive with natural ketoreductases.⁶ The reaction is performed at pH 7.0 and 30 °C without co-solvent and at high initial substrate loading which is the strength of this reaction. They reached a yield of 94% with >99.8% ee. They also patented the enzymatic synthesis of a commercial product, (S)-(+)-licarbazepine which is an active metabolite.⁷ A yield of 96% was reached with 99.9% ee by performing the reaction in 60% isopropanol at 55 °C with 100 g/L of substrate. Enzymeworks patented the enzymatic synthesis of the intermediate of duloxetine which is an antidepressant.⁸ They reached a yield of 96% with 99.9% ee, by carrying out the reaction with 220 g/L of substrate and 0.05 g/L of NADP, which represent an impressive $TON_{(NADP)}$ of more than 17,000. Finally, for demonstrating that all challenges are not completely overcome, a medicinal chemistry group from Pfizer presents an enzymatic reduction done in 10% of isopropanol.⁹ Due to the purification by crystallisation, half of the product is lost.

The examples in Table 1.1 give a good overview of the state-of-the-art in industrially implemented biocatalytic reductions. All these reactions still need stoichiometric amounts of reductants (isopropanol, etc.) and catalytic quantities of cofactors. For a truly green and simpler process the circumvention of cofactors or photoregeneration thereof would be a large step forward. The energy would in this case be provided by light. In the next paragraphs we discuss the state-of-the-art in enzymatic oxidation and reduction reaction and how the use of light could advance the applicability of these reactions even further.

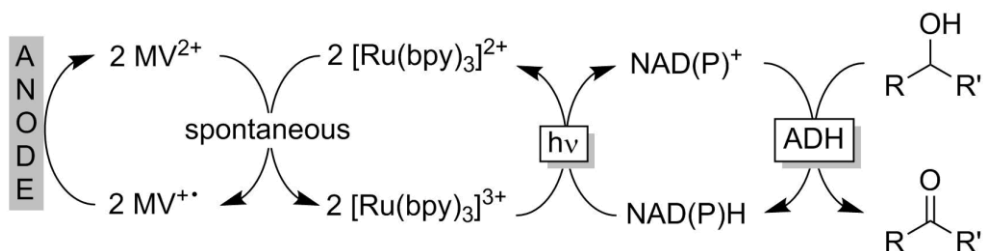
The central role of NAD(P) as electron donor and acceptor in biocatalytic redox reactions has motivated researchers to develop *in situ* regeneration systems to allow for the use of these costly cofactors in catalytic amounts and thereby reduce their cost contribution to the desired product.¹⁰

The number of enzymatic regeneration systems of NAD(P)⁺ however is low and falls back significantly behind the number of NAD(P)H regeneration systems. In essence, NADH-oxidases¹¹⁻¹⁴ and ADH-catalysed NAD(P)H oxidation¹⁵⁻¹⁸ prevail. Nevertheless, a range of photochemical NAD(P)⁺ regeneration systems has been reported. In contrast to the reverse reaction (photochemical reduction of NAD(P)⁺), selectivity issues play no role in the reaction mixtures as the desired product (NAD(P)⁺) is aromatic and thereby thermodynamically stable (Scheme 1.1).



Scheme 1.1. Structure of nicotinamide cofactors (A) and ECE mechanism of NAD(P)H oxidation (B).

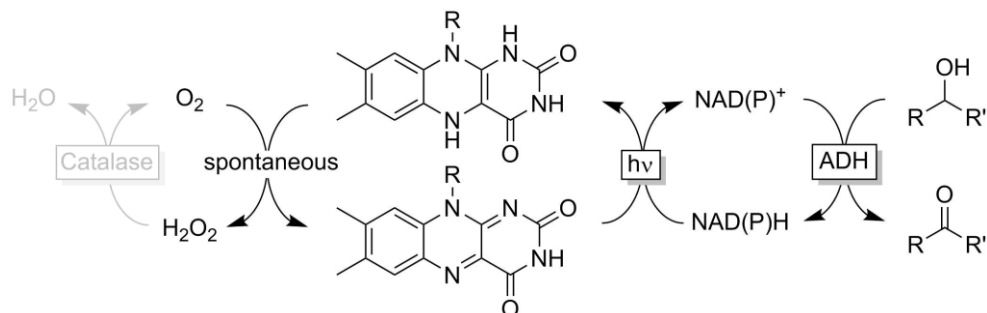
In an early contribution, Steckhan and coworkers reported a photoelectrochemical NAD(P)H oxidation system based on photoexcited $[\text{Ru}(\text{bpy})_3]^{3+}$ complexes (Scheme 1.2).¹⁹ The reducing equivalents transferred to the photoexcited Ru complexes were then, in a spontaneous cascade, transferred to an anode. Unfortunately, this system proved to be rather complex and not efficient enough to be of preparative use.



Scheme 1.2. The photoelectrochemical NAD(P)⁺ regeneration system proposed by Steckhan and coworkers to promote ADH-catalysed oxidation reactions.

Later, we reported that photoexcited flavins are very efficient catalysts to oxidise NAD(P)H to NAD(P)⁺.^{20,21} The spontaneous hydride transfer from NAD(P)H to oxidised flavins is actually known since decades.²²⁻²⁵ The sluggish reaction rate, however, demanded large molar surpluses of the flavin 'catalyst' to achieve acceptable overall reaction rates. Simple illumination of the reaction system with blue light ($\lambda=450$ nm, i.e. the absorption maximum of oxidised flavins) increased

the reaction rate by orders of magnitude thereby enabling truly catalytic use of the flavin photocatalyst (Scheme 1.3). This approach is also applicable to various other photoactive redox dyes such as methylene blue, rose Bengal or Meldola's blue.²⁶



Scheme 1.3. Photochemical NAD(P)^+ regeneration system using photoexcited flavins. Please note, the mechanism shown here is highly simplified. Most likely, flavin-semiquinone radicals formed by SET from NAD(P)H to the photoexcited flavin are formed, reacting with O_2 in a sequence of SETs.²⁷

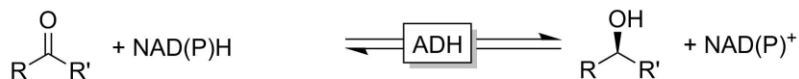
Principally, reductive regeneration of redox enzymes can be achieved either directly, i.e. by direct reduction of the enzymes' active sites or indirectly, i.e. involving the nicotinamide cofactors. Both approaches will be outlined in the following sections.

The Old Yellow Enzyme (OYE) family of flavoproteins is able to selectively reduce the C=C-double bond of α,β -unsaturated ketones and aldehydes. This enzyme family has been studied extensively during almost a century.

The reduced nicotinamide cofactors NADH and NADPH play a pivotal role as electron donors in many biocatalytic redox reactions (Scheme 1.4). For their *in situ* regeneration, enzymatic regeneration systems prevail. This is mainly due to their inherent compatibility with the enzymatic production systems but also due to the ease of application. The most common systems are shown in Scheme 1.5.

Reduction reactions

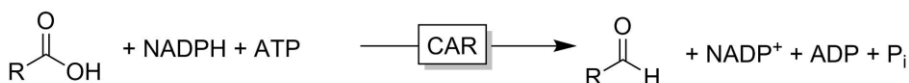
Reduction of aldehydes and ketones



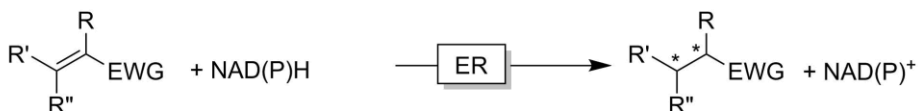
Reductive amination of aldehydes and ketones



Reduction of carboxylic acids



Reduction of conjugated C=C-double bonds

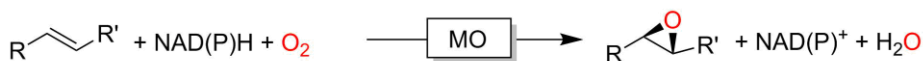


Oxidation reactions

Baeyer-Villiger oxidation reactions



Epoxidation of C=C-double bonds



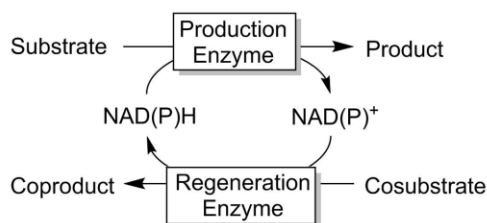
Hydroxylation of C-H-bonds



Heteroatom oxidations



Scheme 1.4. Selection of preparatively relevant NAD(P)H-dependent redox reactions. ADH: alcohol dehydrogenase, IRED: imine reductase, CAR: carboxylic acid reductase, ER: ene reductase, BVMO: Bayer-Villiger monoxygenase, MO: monoxygenase (general).



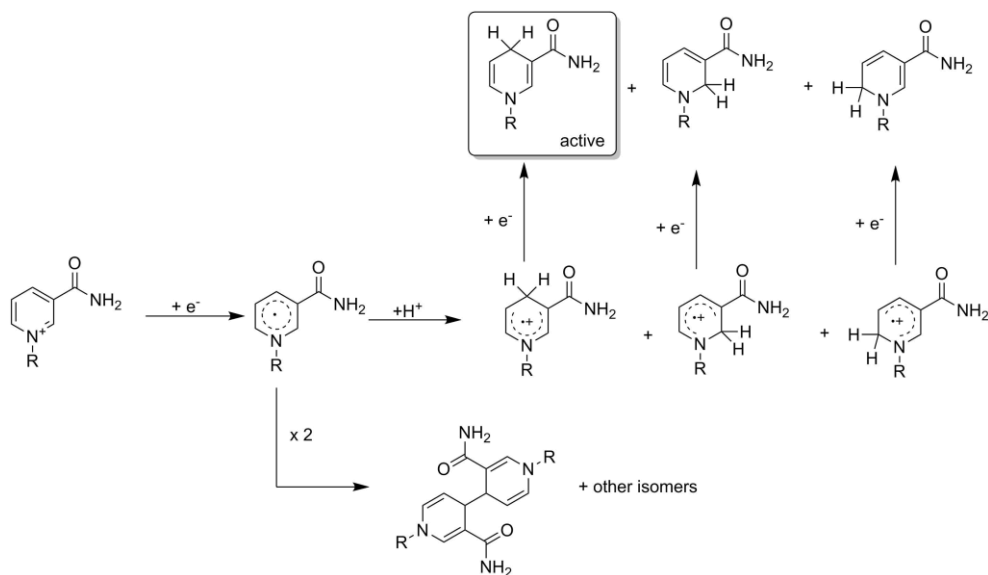
Regeneration Enzyme	Cosubstrate	Coproduct
Formate dehydrogenase (FDH)	HCO_2H	CO_2
Alcohol dehydrogenase (ADH)	$\begin{array}{c} \text{OH} \\ \\ \text{R}-\text{C}-\text{R}' \end{array}$	$\begin{array}{c} \text{O} \\ \\ \text{R}-\text{C}-\text{R}' \end{array}$
Glucose dehydrogenase (GDH)		
Phosphite dehydrogenase (PDH)	H_3PO_3	H_3PO_4
Hydrogenase (HAse)	H_2	-

Scheme 1.5. Selection of common enzymatic NAD(P)H regeneration systems.

Another reason for the dominance of enzymatic regeneration systems lies in their intrinsic regioselectivity. The reduction of NAD(P)^+ to NAD(P)H can principally lead to three different regioisomers of NAD(P)H while only the 1,4- NAD(P)H can be used by the production enzyme. Hence, a successful NAD(P)H regeneration system must be highly selective otherwise, losses in the costly nicotinamide cofactor due to formation of inactive regioisomers will make the approach economically unattractive.²⁸

Unfortunately, the majority of photocatalysts follow a so-called ECE (electron transfer – chemical – electron transfer) mechanism resulting in two major issues for the selective formation of 1,4- NAD(P)H . First, the intermediate NAD^{\cdot} -radical can dimerise (comprising yet another pathway to inactivate the nicotinamide cofactor).

Second, the chemical protonation step seldom is regioselective leading to the formation of the undesired NAD(P)H isomers (Scheme 1.6).²⁹



Scheme 1.6. ECE mechanism of NAD(P)⁺ reduction and its consequences for the formation of NAD(P)-dimers and NAD(P)H isomers.

To circumvent (or at least alleviate) the loss of enzyme-active 1,4-NAD(P)H due to direct single electron reduction by the reduced photocatalyst, generally a relay system is applied to convert the ECE-steps into a regioselective hydride transfer step. The organometallic complex [Cp*₃Rh(bpy)(H₂O)]²⁺ proposed by Steckhan³⁰⁻³⁵ or NAD(P)H:flavin oxidoreductases³⁶⁻⁴⁰ are the most frequently used for this purpose:

Table 1.2. Selection of indirect photochemical NAD(P)H regeneration systems.

Cosubstrate	Photocatalyst	Production enzyme / Product (final con. [mM])	TN (NAD(P))	TN (Catalysts)	Ref
[Cp*Rh(bpy)(H₂O)]²⁺ as relay system²⁶					
TEOA	CNR	GluDH / Glutamate (10)	10	Rh: 20 CNR: n.d. GluDH: n.d.	41
TEOA	mCNS	LacDH / Lactate (5)	5	Rh: 20 mCNS: n.d. LacDH: n.d.	42
TEOA	Eosin Y	GluDH / Glutamate (10)	200	Rh: 40 Eosin Y: 500 GluDH: n.d.	43,44
TEOA	[Ru(bpy) ₃] ²⁺	GluDH / Glutamate (5)	5		45
H ₂ O	[Co ₄ (H ₂ O) ₂ (PW ₉ O ₃₄) ₂] ¹⁰⁻	GluDH / Glutamate (5)	1.5		45
TEOA	Chemically converted graphene	<i>Lb</i> ADH / Various alcohols (<10 mM)	15	Rh: 30	46,47
TEOA	Chemically converted graphene	FDH / HCO ₂ H	116	Rh: 232	48-50
	Hydrogen-Terminated Silicon Nanowires	GluDH / Glutamate (5)	4	Rh: 20	51
NAD(P)H:flavin oxidoreductases as a relay system					
Ascorbic acid	Quantum dots	<i>Tb</i> ADH / Isobutanol	8	FNR: 3167	38
EDTA	DRf	ADH-A / Chiral alcohols (<5 mM)	21	PDR: 870 DRf: 72 MV: 17	36

TEOA: triethanolamine; CNR: graphitic carbonitride nanorods; mCNS: mesoporous carbonitride spheres; LacDH: lactate dehydrogenase; GluDH: glutamate dehydrogenase; FDH: formate dehydrogenase; DRf: 5-deazariboflavin; MV: methyl viologen.

A selection of photochemical NAD(P)H regeneration systems used to promote biocatalytic reduction reactions is summarised in Table 1.2. Although various photocatalysts and relay systems have been reported in the past ten years, the overall NAD(P) turnover numbers and the product concentrations achieved so far

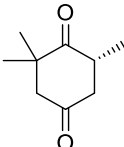
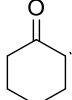
are disappointing. Compared to the multiple thousands (even millions) of turnovers reported regeneration systems with enzymes, the current performance falls back by orders of magnitude.

Significant improvements will be necessary in the nearer future to make photochemical NAD(P)H regeneration systems a viable alternative (rather than a lab curiosity) to existing enzymatic systems.

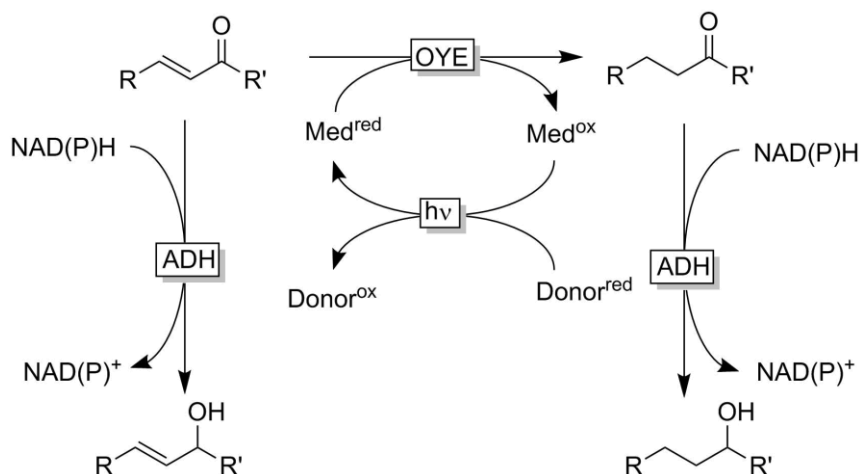
Flavin-dependent old yellow enzymes (OYEs), for example, have been in focus of direct photochemical regeneration for some time now. Flavins exhibit a more flexible redox chemistry especially if compared to the aforementioned nicotinamide cofactors. Therefore, flavoenzymes appear more suitable for direct (not including NAD(P)H) regeneration e.g. by reduced photosensitisers. A selection of recent examples comprising photochemical regeneration of OYEs is listed in Table 1.3.

One advantage of the NAD(P)H-independent, direct regeneration of OYE is that the costly and instable nicotinamide cofactor (together with an enzymatic regeneration system) can be omitted from the reaction scheme. Furthermore, photochemical OYE-regeneration systems do not regenerate the nicotinamide cofactor. Thus, NAD(P)H-dependent enzymes, possibly present in cell-free extracts, are not regenerated and possible side-reactions such as ketoreduction are avoided. To achieve this chemoselectivity with traditional regeneration schemes, highly purified enzyme preparations (devoid of any ADHs) are required. Hence, photochemical, direct regeneration of OYE not only offers the opportunity of saving costs by omitting the nicotinamide cofactor (and its regeneration system) but also for products of higher purity due to the high chemoselectivity of the reaction (Scheme 1.7).

Table 1.3. Selected example of C=C-bond reductions using photochemically regenerated OYEs.

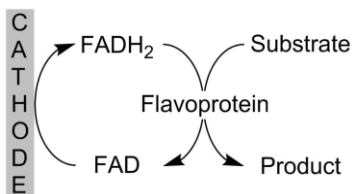
Product	Cosubstrate	OYE	Photocatalyst	Mediator	TN (OYE / Photocatalyst / Mediator)	ref
	EDTA	YqjM	FMN	FMN	10900 / 1000	52,53
	TEOA	YqjM	CdSe	MV ²⁺	n.d.	54
	MOPS / H ₂ O	YqjM	Au-TiO ₂	FMN	650 / n.d. / 50	55
	Cathode	TsOYE	Flavin-modified CNT-cathode	-	230 / 2	56
	EDTA	TsOYE	Rose bengal	-	250 / 40	57
		DrER & RmER	FMN	-	2080 / 16	58
HO ₂ C-CH ₂ -CO ₂ H	H ₂ O	Flavocytochrome c (fcc ₃)	TiO ₂ -modified FTO anode for water oxidation	-	n.d.	59

YqjM: OYE from *Bacillus subtilis*; TsOYE: OYE from *Thermus scotoductus*; FTO: fluorine-doped tin oxide; MV: methyl viologen; FMN: flavin mononucleotide.



Scheme 1.7. Increased chemoselectivity of OYE-catalysed reduction of conjugated C=C-double bond via direct, NAD(P)H-independent regeneration of the flavin-prosthetic group. 'Contaminating' alcohol dehydrogenases (ADHs) catalysing the carbonyl reduction of both, the starting material and the products are not regenerated and therefore remain inactive.

Direct electrochemical regeneration of enzymes is impeded due to their buried catalytic site which hindered direct contact between the enzyme and the cathode. Therefore, mediators are used to transfer electrons from the cathode to the enzyme's active site, such as viologens,⁶⁰ cobalt sepulchrates,⁶¹ ferrocenes^{62,63} and flavins^{64,65}. Electrochemical regenerations of reduced FADH_2 have been reported for the regeneration of flavoproteins, such as StyA (Scheme 1.8)^{66,67}.



Scheme 1.8. Electrochemical regeneration of flavins for the regeneration of flavoproteins

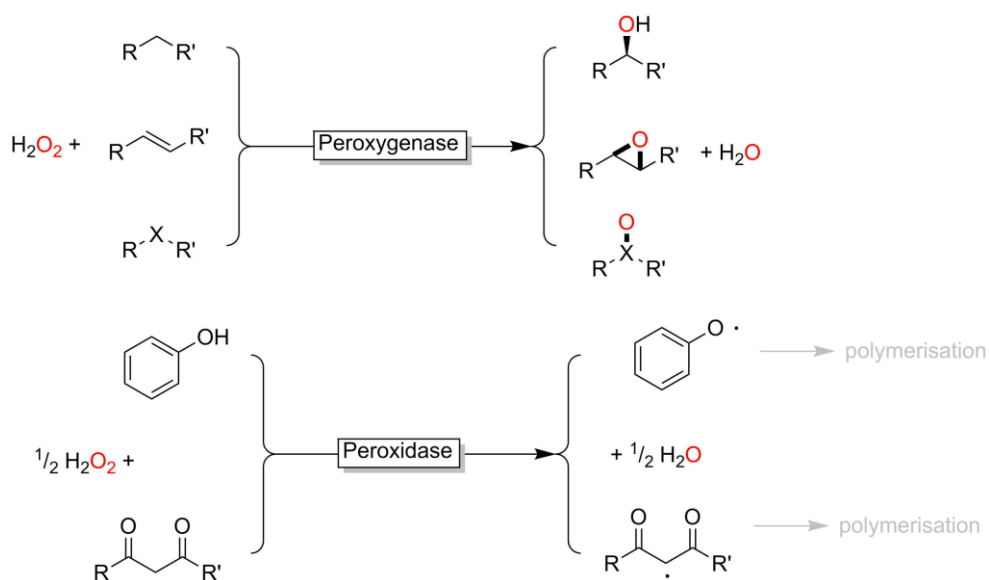
Instead of using the metal as an electrode which is surface-limited, elementary metal powder can also be used for regenerating mediators. Schwaneberg *et al.* published the regeneration of reduced cobalt sepulchrates with cheap zinc powder for the regeneration of P450 BM-3.⁶⁸ This alternative can be used instead of expensive electrochemical devices such as platinum electrodes.

Zinc dust has also been chosen as electron donor for regenerating artificial flavins modified on the isoalloxazine ring.⁶⁹⁻⁷⁰ With these flavins, researchers are aiming to mimic flavoproteins such as Bayer-Villiger monooxygenase. By simulating the enzymatic function of flavins, molecular oxygen is converted into synthetic flavin hydroperoxides. Elementary metal powder has the advantage of a quasi-unlimited surface area for reducing mediators, but so far this approach has not found widespread and systematic investigation in research.

A reaction of particular interest is the epoxidation reaction. Recently, peroxygenases have been disclosed as the enzymes of choice for this reaction, because of their high activity, stability and wide substrate scope. In this case, hydrogen peroxide is the oxidation reagent, which from a green perspective is an acceptable choice. For upscaling however, the use of pure organic solvent would mean a large step.

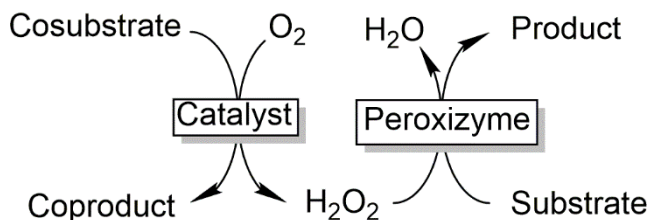
Peroxygenases are NAD(P)H-independent enzymes and excel in terms of specific activity compared to the well-known P450 monooxygenase. In contrast with P450, peroxygenases rely on a simpler electron transport chains for the reduction of the haem active site. They utilise H_2O_2 , which is a cheap compound, to generate active oxyferryl haem species.⁷¹ One of their major pitfalls so far is their instability toward peroxides. *In situ* formation of peroxide has been chosen to be the solution of this issue.

Photochemical systems in the presence of molecular oxygen tend to uncouple. Indeed, the reduced photocatalysts/mediators (mostly being radicals) react swiftly with molecular oxygen directly. In the case of photochemical NAD(P)⁺ regeneration systems, this is the desired reaction. In cases where the reducing equivalents should be delivered to a biocatalyst (i.e. to a monooxygenase), this represents an undesired side reactions. In some cases, this side reaction dominates over the desired electron flow leading to a waste of up to 95% of the reducing equivalents (Oxygen Dilemma).⁷² The final product of this uncoupling reaction is H_2O_2 , which can be used to promote peroxygenases-mediated oxidations.



Scheme 1.9. Peroxizymes utilise H_2O_2 to catalyse or initiate catalytic oxidation reactions.

Peroxygenases (UPO for unspecific peroxygenases) catalyse a very broad range of synthetically useful oxyfunctionalisation reactions such as regio- and stereospecific hydroxylations and epoxidations as well as stereospecific heteroatom oxygenations (Scheme 1.9). As heme-dependent enzymes, however, they are also prone to rapid oxidative inactivation in the presence of H_2O_2 as mentioned above.⁷³ Therefore, a range of *in situ* H_2O_2 generation approaches have been developed in the past to balance the H_2O_2 concentration to the UPO activity and thereby minimise oxidative inactivation.⁷¹ Most prominent at present, are enzymatic systems based on oxidases (i.e. enzymes that couple the oxidation of their substrate to the reduction of O_2 to H_2O_2). In the past decade, we and others have developed a range of photocatalytic systems to drive peroxygenase- and peroxidase-reactions. A summary is given in Table 1.4.

Table 1.4. Selection of peroxidase reactions driven by photocatalytic H₂O₂ generation.

Catalyst	Cosubstrate	Coproduct	Peroxidase	Product	TTN (Enzyme)	Remarks	ref
Flavin	EDTA	EDTriA / H ₂ CO / CO ₂	<i>CfCPO</i>	thioanisole sulfoxide	22000	Using a 2LPS approach significantly improved product formation	74,75
Flavin	EDTA	EDTriA / H ₂ CO / CO ₂	<i>AaeUPO</i>	various	<40000		76
Flavin	EDTA	EDTriA / H ₂ CO / CO ₂	<i>OleT</i>	1-alkenes			77,78
Flavin- modified cathode	H ₂ O	O ₂	<i>AaeUPO</i>	1-phenyl ethanol	123000	Photo- electrochemical approach	79
Au-TiO ₂	MeOH	CO ₂	<i>AaeUPO</i>	various	>60000		80
Au-TiO ₂	H ₂ O	O ₂	<i>AaeUPO</i>	various	>30000		81
Various dyes / FDH	HCO ₂ H	CO ₂	<i>AaeUPO</i>	1-phenyl ethanol	>40000	Combining color- complementary redox dyes allows better usage of the visible light range	82
Flavin	EDTA	EDTriA / H ₂ CO / CO ₂	cytochrome P450 peroxygenases	Hydroxy myristic acid	200	Low, due to poor solubility of the reagents	83
Flavin	MES	n.d.	<i>AmVHCPO</i>	Various halogenated phenols and anilines	2000		84

EDTA: ethylenediamine tetraacetate; EDTriA: ethylenediamine triacetate; MES: 2-(N-morpholino)ethanesulfonic acid; *AmVHCPO*: V-dependent haloperoxidase from *Acryochloris marina*.

Obviously, using water as cosubstrate would be the most attractive application of photocatalysis with peroxygenases from a cost-effective point of view for its high atom efficiency. However the current state-of-the-art is hampered by the rather sluggish water oxidation rates making the resulting reaction systems rather slow.

In conclusion, the systems in Table 1.4 still do not lead to the desired activity. Therefore in this thesis, another approach was taken to reach a next level in upscaling peroxygenases, namely by performing the reaction under neat organic solvent conditions.

In this thesis, three systems have thus been studied. We characterised them with the purpose of bringing them to preparative scale.

1. G. Torreló, U. Hanefeld, F. Hollmann. *Biocatalysis. Catal. Lett.*, 2015, **145**, 309-345.
2. K. Faber, *Biotransformations in Organic Chemistry*, Springer, Berlin, 6th ed., 2011.
3. K. Drauz, H. Groeger, O. May, eds. *Enzyme Catalysis in Organic Synthesis. Weinheim: Wiley-VCH*, 2012.
4. A. Liese, K. Seelbach, C. Wandrey, *Industrial Biotransformations. Weinheim: Wiley-VCH*, 2006.
5. D.L. Hughes, *Org. Process Res. Dev.*, 2018, **22**, 1063-1080.
6. J. Liang, S.J. Jenne, E. Mundorff, C. Ching, J.M. Gruber, A. Krebber, G.W. Huisman, U.S. Patent Application 2017/0067032 A1, March 9, 2017.
7. A. Gohel, D.J. Smith, B. Wong, J. Sukumaran, W.L. Yeo, S.J. Collier, S. Novick, U.S. Patent Application 2017/0159028 A1, June 8, 2017.
8. M. Fu, T. Zhang, Chinese Patent Application CN 106011096, Oct 12, 2016.
9. M.Y. Pettersson, D.S. Johnson, C. Subramanyam, J. O'Donnell, W. am Ende, M.E. Green, N.C. Patel, C.M. Stiff, T.P. Tran, G.W. Kauffman, A.F. Stepan, P.R. Verhoest, U.S. Patent Application 2016/0024088 A1, Jan 28, 2016.
10. H. Chenault, G. Whitesides, *App. Biochem. Biotechnol.*, 1987, **14**, 147-197.
11. J.T. Park, J-I. Hirano, V. Thangavel, B.R. Riebel, A.S. Bommarius. *J. Mol. Catal. B: Enzym.*, 2011, **71**, 159-165.
12. R. Jiang, A.S. Bommarius. *Tetrahedron Asymm.*, 2004, **15**, 2939-2944.
13. B.R. Riebel, P.R. Gibbs, W.B. Wellborn, A.S. Bommarius, *Adv. Synth. Catal.*, 2003, **345**, 707-712.
14. B.R. Riebel, P.R. Gibbs, W.B. Wellborn, A.S. Bommarius, *Adv. Synth. Catal.*, 2002, **344**, 1156-1168.
15. C.E. Paul, I. Lavandera, V. Gotor-Fernández, W. Kroutil, V. Gotor, *ChemCatChem* 2013, **5**, 3875–3881.
16. T. Orbegozo, I. Lavandera, W.M.F. Fabian, B. Mautner, J.G. de Vries, W. Kroutil, *Tetrahedron*, 2009, **65**, 6805-6809.
17. I. Lavandera, A. Kern, V. Resch, B. Ferreira-Silva, A. Glieder, W.M.F. Fabian, S. de Wildeman, W. Kroutil, *Org. Lett.*, 2008, **10**, 2155-2158.
18. W. Kroutil, H. Mang, K. Edegger, K. Faber, *Adv. Synth. Catal.*, 2004, **346**, 125-142.
19. R. Ruppert, E. Steckhan, *J. Chem. Soc.-Perkin Trans. 2*, 1989, 811-814.
20. S. Gargiulo, I.W.C.E. Arends, F. Hollmann, *ChemCatChem*, 2011, **3**, 338-342.

21. M. Rauch, S. Schmidt, I.W.C.E. Arends, K. Oppelt, S. Kara, F. Hollmann, *Green Chem.*, 2017, **19**, 376-379.
22. J.B. Jones, K.E. Taylor, *Can. J. Chem.*, 1976, **54**, 2969-2973.
23. F. Boratyński, K. Dancewicz, M. Paprocka, B. Gabryś, C. Wawrzeńcz, *PLoS One*, 2016, **11**, e0146160.
24. F. Boratynski, M. Smuga, C. Wawrzenczyk, *Food Chem.*, 2013, **141**, 419-427.
25. F. Boratynski, G. Kielbowicz, C. Wawrzenczyk, *J. Mol. Catal. B Enzym.*, 2010, **65**, 30-36.
26. S. Kochius, Y. Ni, S. Kara, S. Gargiulo, J. Schrader, D. Holtmann, F. Hollmann, *ChemPlusChem*, 2014, **79**, 1554-1557.
27. V. Massey, *J. Biol. Chem.*, 1994, **269**, 22459-22462.
28. E. Steckhan, *Electrochemistry V. Berlin 33: Springer-Verlag Berlin*, 1994, 83-111.
29. F. Hollmann, A. Schmid, *Biocatal. Biotransf.*, 2004, **22**, 63-88.
30. E. Steckhan, S. Herrmann, R. Ruppert, J. Thommes, C. Wandrey, *Angew. Chem. Int. Ed.*, 1990, **29**, 388-390.
31. R. Ruppert, S. Herrmann, E. Steckhan, *J. Chem. Soc.-Chem. Commun.*, 1988, 1150-1151.
32. S. Grammenudi, M. Franke, F. Vogtle, E. Steckhan, *J. Incl. Phenom.*, 1987, **5**, 695-707.
33. R. Wienkamp, E. Steckhan, *Angew. Chem. Int. Ed.*, 1983, **22**, 497.
34. R. Wienkamp, E. Steckhan, *Angew. Chem. Int. Ed.*, 1982, **21**, 782-783.
35. F. Hollmann, B. Witholt, A. Schmid, *J. Mol. Catal. B: Enzym.*, 2002, **19-20**, 167-176.
36. G.T. Höfler, E. Fernández-Fueyo, M. Pesic, S.H. Younes, E.-G. Choi, Y.H. Kim, V.B. Urlacher, I.W.C.E. Arends, F. Hollmann, *ChemBioChem*, 2018, **19**, 2344-2347.
37. L. Wan, C.F. Megarity, B. Siritanaratkul, F.A. Armstrong, *Chem. Commun.*, 2018, 54, 972-975.
38. K.A. Brown, M.B. Wilker, M. Boehm, H. Hamby, G. Dukovic, P.W. King, *ACS Catal.*, 2016, **6**, 2201-2204.
39. H. Asada, T. Itoh, Y. Kodera, A. Matsushima, M. Hiroto, H. Nishimura, Y. Inada, *Biotechnol. Bioeng.*, 2001, **76**, 86-90.
40. J.J. Pueyo, C. Gomezmoreno, *Enz. Microb. Technol.*, 1992, **14**, 8-12.
41. J. Liu, J. Huang, H. Zhou, M. Antonietti, *ACS Appl. Mater. Interfaces*, 2014, **6**, 8434-8440.
42. J.H. Huang, M. Antonietti, J. Liu, *J. Mater. Chem. A*, 2014, **2**, 7686-7693.
43. S.H. Lee, D.H. Nam, C.B. Park, *Adv. Synth. Catal.*, 2009, **351**, 2589-2594.
44. S.H. Lee, D.H. Nam, J.H. Kim, J.-O. Baeg, C.B. Park, *ChemBioChem*, 2009, **10**, 1621-1624.
45. J. Ryu, D.H. Nam, S.H. Lee, C.B. Park, *Chem. Eur. J.*, 2014, **20**, 12020-12025.
46. S. Choudhury, J.-O. Baeg, N.-J. Park, R.K. Yadav, *Green Chem.*, 2014, **16**, 4389-4400.
47. S. Choudhury, J.O. Baeg, N.J. Park, R.K. Yadav, *Angew. Chem. Int. Ed.*, 2012, **51**, 11624-11628.
48. R.K. Yadav, J.O. Baeg, A. Kumar, K.J. Kong, G.H. Oh, N.J. Park, *J. Mater. Chem. A*, 2014, **2**, 5068-5076.
49. R.K. Yadav, G.H. Oh, N.J. Park, A. Kumar, K.J. Kong, J.O. Baeg, *J. Am. Chem. Soc.*, 2014, **136**, 16728-16731.

50. R.K. Yadav, J.O. Baeg, G.H. Oh, N.-J. Park, K.-J. Kong, J. Kim, D.W. Hwang, S.K. Biswas, *J. Am. Chem. Soc.*, 2012, **134**, 11455-11461.
51. H.Y. Lee, J. Ryu, J.H. Kim, S.H. Lee, C.B. Park, *ChemSusChem*, 2012, **5**, 2129-2132
52. A. Taglieber, F. Schulz, F. Hollmann, M. Rusek, M.T. Reetz, *ChemBioChem*, 2008, **9**, 565-572.
53. M. Mifsud Grau, J.C. van der Toorn, L.G. Otten, P. Macheroux, A. Taglieber, F.E. Zilly, I.W.C.E. Arends, F. Hollmann, *Adv. Synth. Catal.*, 2009, **351**, 3279-3286.
54. T.N. Burai, A.J. Panay, H. Zhu, T. Lian, S. Lutz, *ACS Catal.*, 2012, **2**, 667-670.
55. M. Mifsud, S. Gargiulo, S. Iborra, I.W.C.E. Arends, F. Hollmann, A. Corma, *Nat. Commun.*, 2014, **5**, 3145.
56. E.J. Son, S.H. Lee, S.K. Kuk, M. Pesic, D.S. Choi, J.W. Ko, K. Kim, F. Hollmann, C.B. Park, *Adv. Funct. Mater.*, 2018, **28**, 1705232.
57. S.H. Lee, D.S. Choi, M. Pesic, Y.W. Lee, C.E. Paul, F. Hollmann, C.B. Park, *Angew. Chem. Int. Ed.*, 2017, **56**, 8681-8685.
58. S. Litthauer, E. van Heerden, D.J. Opperman, S. Gargiulo, F. Hollmann, *J. Mol. Catal. B: Enzym.*, 2014, **99**, 89-95.
59. A. Bachmeier, B.J. Murphy, F.A. Armstrong, *J. Am. Chem. Soc.*, 2014, **136**, 12876-12879.
60. J.S. Bus, S.D. Aust, J.E. Gibson, *Environ. Health Perspect.*, 1976, **16**, 139-146.
61. M. Schulz, H. Leichmann, H. Günther, H. Simon, *Appl. Microbiol. Biotechnol.*, 1995, **45**, 916-922.
62. C. Ramirez-Molina, M. Boujtita, N. El Murr, *Electroanalysis*, 2003, **15**, 1095-1100.
63. H.-Z. Bu, S.R. Mikkelsen, A.M. English, *Anal. Chem.*, 1998, **70**, 4320-4325.
64. M.H. Kim, S.E. Yun, *Biotechnol. Lett.*, 2004, **26**, 21-26.
65. S. Cosnier, M. Fontecave, C. Innocent, V. Niviere, *Electroanalysis*, 1997, **9**, 685-688.
66. F. Hollmann, K. Hofstetter, T. Habicher, B. Hauer, A. Schmid, *J. Am. Chem. Soc.*, 2005, **127**, 6540-6541.
67. R. Ruinatscha, C. Dusny, K. Buehler, A. Schmid, *Adv. Synth. Catal.*, 2009, **351**, 2505-2515.
68. U. Schwaneberg, D. Appel, J. Schmitt, R.D. Schmid, *J. Biotechnol.*, 2000, **84**, 249-257.
69. Y. Imada, H. Iida, S.-I. Murahashi, T. Naota, *Angew. Chem. Int. Ed.*, 2005, **44**, 1704-1706.
70. Y. Arakawa, K. Yamanomoto, H. Kita, K. Minagawa, M. Tanaka, N. Haraguchi, S. Itsuno, Y. Imada, *Chem. Sci.*, 2017, **8**, 5468.
71. B.O. Burek, S. Bormann, F. Hollmann, J.Z. Bloh, D. Holtmann, *Green Chem.*, 2019, **21**, 3232-3249.
72. D. Holtmann, F. Hollmann, *ChemBioChem*, 2016, **17**, 1391-1398.
73. B. Valderrama, M. Ayala, R. Vazquez-Duhalt, *Chem. Biol.*, 2002, **9**, 555-565.
74. D.I. Perez, M. Mifsud Grau, I.W.C.E. Arends, F. Hollmann, *Chem. Commun.*, 2009, **44**, 6848-6850.
75. E. Churakova, I.W.C.E. Arends, F. Hollmann, *ChemCatChem*, 2013, **5**, 565-568.
76. E. Churakova, M. Kluge, R. Ullrich, I.W.C.E. Arends, M. Hofrichter, F. Hollmann, *Angew. Chem. Int. Ed.*, 2011, **50**, 10716-10719.

77. I. Zachos, S. Gassmeyer, D. Bauer, V. Sieber, F. Hollmann, R. Kourist, *Chem. Commun.*, 2015, **51**, 1918-1921.
78. S. Bojarra, D. Reichert, M. Grote, A. Gomez Baraibar, A. Dennig, B. Nidetzky, C. Mügge, R. Kourist, *ChemCatChem*, 2018, **10**, 1192-1201.
79. D.S. Choi, Y. Ni, E. Fernández-Fueyo, M. Lee, F. Hollmann, C.B. Park, *ACS Catal.*, 2017, **7**, 1563-1567.
80. W. Zhang, B.O. Burek, E. Fernández-Fueyo, M. Alcalde, J.Z. Bloh, F. Hollmann, *Angew. Chem. Int. Ed.*, 2017, **56**, 15451–15455.
81. W. Zhang, E. Fernández-Fueyo, Y. Ni, M. van Schie, J. Gacs, R. Renirie, R. Wever, F.G. Mutti, D. Rother, M. Alcalde, F. Hollmann, *Nat. Catal.*, 2018, **1**, 55–62.
82. S.J.-P. Willot, E. Fernández-Fueyo, F. Tieves, M. Pesic, M. Alcalde, I.W.C.E. Arends, C.B.Park, F. Hollmann, *ACS Catal.*, 2019, **9**, 890-894.
83. M. Girhard, E. Kunigk, S. Tihovsky, V.V. Shumyantseva, V.B. Urlacher, *Biotechnol. Appl. Biochem.*, 2013, **60**, 111-118.
84. C.J. Seel, A. Králík, M. Hacker, A. Frank, B. König, T. Gulder, *ChemCatChem*, 2018, **10**, 3960-3963.

2LPS: two liquid phases system
AaeUPO: unspecific peroxygenase from *Agrocybe aegerita*
ADH: alcohol dehydrogenase
AmVHCPO: V-dependent haloperoxidase from *Acaryochloris marina*
BVMO: Bayer-Villiger monooxygenase
CAR: carboxylic acid reductase
CfCPO: chloroperoxidase from *Caldariomyces fumago*
CNR: graphitic carbonitride nanorods
CNT: carbon nanotube
DRf: 5-deazariboflavin
ECE: electron transfer – chemical – electron transfer
EDTA: ethylenediaminetetraacetic acid
EDTriA: ethylenediamine triacetate
ER: ene reductase
EWG: electron withdrawing group
FAD: flavin adenine dinucleotide
FDH: formate dehydrogenase
FMN: flavin mononucleotide
FNR: ferredoxin NADP⁺-reductase
FTO: fluorine-doped tin oxide
GDH: glucose dehydrogenase
GluDH: glutamate dehydrogenase
Hase: hydrogenase
HLADH: horse liver alcohol dehydrogenase
IRED: imine reductase
LacDH: lactate dehydrogenase
mCNS: mesoporous carbonitride spheres
MO: monooxygenase
MV: methyl viologen
NAD(P)⁺: oxidised form of the (phosphorylated) nicotinamide adenine dinucleotide cofactor
NAD(P)H: reduced form of the (phosphorylated) nicotinamide adenine dinucleotide cofactor
OleT: P450 fatty acid decarboxylase from *Jeotgalicoccus* sp. ATCC 8456
OYE: old yellow enzyme
PDH: phosphite dehydrogenase
PDR: putidaredoxin reductase
Rf: riboflavin
SET: single-electron transfer
StyA: styrene monooxygenase from *Pseudomonas* sp.
TEOA: triethanolamine

TN: turnover number

TsOYE: OYE from *Thermus scotoductus*

TTN: total turnover number

UPO: unspecific peroxygenase

YqjM: OYE from *Bacillus subtilis*

Chapter 2:

Photobiocatalytic alcohol oxidation using LED light source

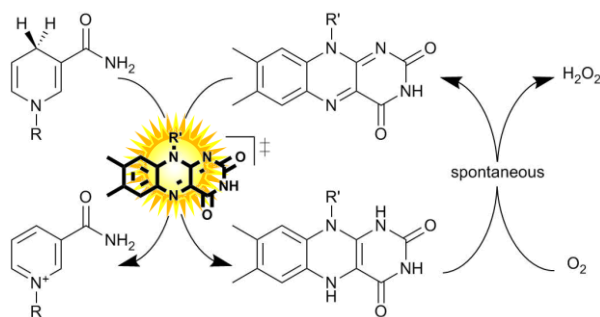
The photocatalytic oxidation of NADH using a flavin photocatalyst and a simple blue LED light source is reported. This *in situ* NAD⁺ regeneration system can be used to promote biocatalytic, enantioselective oxidation reactions. Compared to the traditional use of white light bulbs, this method enables very significant reductions in energy consumption and CO₂ emission.

This chapter is based on

M.C.R. Rauch, S. Schmidt, I.W.C.E. Arends, K. Oppelt, S. Kara, F. Hollmann, *Green Chem.*, 2017, **19**, 376-379.

2.1. Introduction

Oxidation reactions employing alcohol dehydrogenases are experiencing an increased interest in the field of biocatalysis.¹⁻⁴ While the toolbox of selective enzymes is growing constantly, the choice of efficient *in situ* regeneration systems of the oxidized nicotinamide cofactors to sustain the catalytic cycle is still comparably limited.⁵ This is particularly true for regeneration systems employing molecular oxygen as a terminal oxidant, which is attractive from the high thermodynamic driving force and the innocuous nature of the by-products.⁶⁻¹² As early as 1973, Jones and coworkers proposed using simple flavins to catalyse the aerobic oxidation of reduced nicotinamide cofactors.¹³ The slow reaction kinetics of the hydride transfer from NAD(P)H to the oxidized isoalloxazine moiety rendered the system impractical as significant molar surpluses of the flavin ‘catalysts’ were necessary to attain full conversion within a reasonable time frame. More recently, we have reported that this limitation (low reaction rates) can be overcome simply by applying visible light to the reaction system.¹¹ The overall rate-limiting hydride transfer step from NAD(P)H to the oxidised flavin could be accelerated by photoexcitation of the flavin catalyst. The oxidised flavin catalyst is regenerated spontaneously through aerobic reoxidation yielding hydrogen peroxide (Scheme 2.1).^{14,15}



Scheme 2.1. Aerobic oxidation of reduced nicotinamide cofactors (NAD(P)H) to the corresponding cofactors (NAD(P)⁺) using photoexcited flavin catalysts. Upon photoexcitation ($\lambda = 450 \text{ nm}$) the redox potential of the oxidised flavin catalyst increases dramatically¹⁶ enabling fast hydride transfer from NAD(P)H to the flavin. The reduced flavin reacts spontaneously in a dark reaction with molecular oxygen.¹⁴

During these proof-of-concept experiments we have utilised a simple, commercially available light-white bulb. Despite its simplicity, this setup severely suffered from

heat generated by the bulb. As a consequence not only a significant amount of electrical power used was deviated into heat generations but also additional cooling of the reaction mixture was necessary to maintain optimal reaction conditions for the enzyme reaction.

With the advent of cheap light emitting diode (LED) light sources, we became interested in using those to promote photobiocatalytic oxidation reactions. Compared to the use of traditional light sources, LEDs bear the promise of double energy efficiency: first, LEDs enable a more efficient conversion of electrical power into light energy (only a narrow range of wavelengths is emitted instead of an entire spectrum containing 'useless' wavelengths) and, second, due to the absence of thermal effects, also less thermostating is needed.

2.2. Material and methods

2.2.1. Chemicals

Unless stated otherwise all chemicals were purchased from Sigma-Aldrich (Steinheim, Germany), New England Biolabs (Ipswich, MA, USA) or Merck (Darmstadt, Germany) in the highest quality available and used without further purification.

2.2.2. Analytics

¹H-NMR spectroscopy:

All measurements were recorded on a Bruker NMR unit (Bruker, Karlsruhe, Germany) at 400 MHz in CDCl₃.

Gas chromatography (GC) analysis:

GC measurements were performed on a Shimadzu GC-14A equipped with a Lipodex E column (50 m x 0.25 mm x 0.25 μm, Macherey & Nagel, Düren, Germany) and flame-ionization detection (FID).

2.2.3. Bacterial strains and plasmids

The plasmid pET28a containing the gene encoding the alcohol dehydrogenase from *Equus caballus* bearing an additional N-terminal His₆-tag was kindly provided by Dr. Doerte Rother (Forschungszentrum Juelich, Juelich, Germany). The plasmid was transformed into the appropriate *E. coli* strain by the heat shock method.¹⁷

2.2.4. Cultivation conditions

Expression of Horse Liver Alcohol Dehydrogenase (HLADH) was carried out by inoculation of 400 mL TB (terrific broth) medium supplied with the appropriate antibiotic (kanamycin) with an overnight culture to give an OD₆₀₀ of 0.05. *E. coli* BL21 (DE3) cells were used as expression host. Cells were grown at 37 °C in baffled shake flasks. HLADH expression was induced at an OD₆₀₀ of 0.6-0.8 with 1.0 mM of Isopropyl β-D-1-thiogalactopyranoside (IPTG). Cultivation was continued at 25 °C for 24 hours. Cells were harvested (centrifugation at 1344 g at 4 °C for 15 min) and washed twice in glycine-NaOH buffer (pH 9.0, 100 mM). The bacterial cell pellet was resuspended in the same buffer to give a wet cell weight (WCW) of 100 g/L and passed through a cell disrupter (Constant Systems) at 2000 psi or directly frozen and freeze-dried afterwards.

2.2.5. Purification of HLADH

For purification, cell pellets obtained as described above were resuspended in 25 mL sodium phosphate buffer (100 mM, 300 mM NaCl, pH 7.5) containing 30 mM imidazole. For cell disruption, the cell suspension was passaged twice through a French pressure cell at 2000 psi. Cell debris was separated from the crude extract by centrifugation at 9000 g for 45 min.

Purification of HLADH was performed using the NGC-1 purifier (BioRad, Berkeley, USA). The filtrated supernatant was applied to a Nickel-NTA column (GE Healthcare, Munich, Germany). After washing the column with a triple volume of 100 mM sodium phosphate buffer containing 300 mM sodium chloride at a flow rate of 1 ml min⁻¹, the protein was eluted with 100 mM sodium phosphate buffer containing 300 mM imidazole and 300 mM sodium chloride. The HLADH containing

fractions were collected. The proteins were desalted by PD-10 columns against 100 mM glycine-NaOH buffer (pH 9.0). Afterwards, the protein solution was concentrated using Amicons (10 kDa cut-off). To determine the protein content of the crude cell extract as well as of the purified and desalted fractions, the Bradford assay was used. Standard curves were made using Bovine Serum Albumin (BSA) in a range of 0.02-2 mg/mL. Samples were measured in triplicates using suitable dilutions.

2.2.6. Synthesis of racemic 4-methyltetrahydro-2H-pyran-2-one

Racemic 4-methyltetrahydro-2H-pyran-2-one was synthesized according to the procedure of Phillips and Graham (2008) in a slightly modified manner.¹⁸ A mixture of *meso*-3-methyl-1,5-pentanediol (205 mmol, 1.215 g) and MnO₂ (17 equiv., 4.8 mol, 20.82 g) in CHCl₃ (50 mL) was stirred under reflux conditions at 55 °C for 48 hours. After 48 hours the reaction mixture was aliquoted (30 mL each) into 50 mL Falcon tubes, centrifuged (10,000 rpm, 5 min), and the precipitate was washed with CHCl₃ (3 x 10 mL each). The solvent was removed under reduced pressure to give a yellowish oily compound (600 mg). ¹H-NMR analysis revealed also the presence of the lactol intermediate (4-methyltetrahydro-2H-pyran-2-ol, 31%). Column chromatography was used for separation with a gradient of ethyl acetate / heptane from 1% to 50% for the ethyl acetate. Pure compounds (317 mg of the lactol with an isolated yield of 26% and 190 mg of the lactone with 16% isolated yield) could be obtained.

4-methyltetrahydro-2H-pyran-2-one : ¹H-NMR: (400 MHz, CDCl₃) δ 1.06 (d, J = 6.3 Hz, 3H), 1.56–1.48 (m, 1H), 1.94–1.86 (m, 1H), 2.14–2.04 (m, 2H), 2.71–2.63 (m, 1H), 4.29–4.22 (m, 1H), 4.44– 4.39 (m, 1H).

2.2.7. Synthesis of (*S*)-4-methyltetrahydro-2H-pyran-2-one by HLADH

The synthesis of (*S*)-4-methyltetrahydro-2H-pyran-2-one was performed as previously reported by Kara et al. (2013).¹⁹ For this, a stock of *meso*-3-methyl-1,5-pentanediol (0.5 M), NAD⁺ stock (25 mM), acetosyringone stock (2 mM), and

HLADH stock (3 gL^{-1}) were freshly prepared in 50 mM Tris-HCl buffer at pH 8. The laccase from *Myceliophthora thermophila* (*Mtlaccase*) was used as delivered (0.2 mM solution). The mixture of *meso*-3-methyl-1,5-pentanediol stock (1 mL), acetosyringone stock (1 mL), NAD^+ stock (0.2 mL) and buffer (6.7 mL) was incubated at 30 °C for 5 min. Finally, *Mtlaccase* (0.1 mL) and HLADH solution (1 mL) were added. The starting concentrations were: 50 mM *meso*-3-methyl-1,5-pentanediol, 0.5 mM NAD^+ , 200 μM acetosyringone, 0.3 gL^{-1} HLADH and 2 μM *Mtlaccase*. The reaction mixture (10 mL) was orbitally shaken at 600 rpm in 50 mL Falcon tubes at 30 °C. Samples (50 μL) were taken at defined time intervals and mixed with 200 μL EtOAc (containing 5 mM acetophenone). The mixture was vortexed and dried over anhydrous MgSO_4 . A conversion of 72% to the enantiopure (*S*)-4-methyltetrahydro-2H-pyran-2-one (*enantiomeric excess* (*ee*) >99% according to GC analysis) was achieved after 16 hours. The reaction mixture (10 mL) was then saturated with NaCl and extracted with EtOAc (3 x 10 mL). After each extraction step the mixture was centrifuged (4000 rpm, 10 min). The collected clear organic phase was dried over anhydrous MgSO_4 and the solvent was removed under reduced pressure to give a yellowish oily compound (39 mg). Purification of the crude product was attempted by column chromatography (Pasteur pipette filled with Silica gel 60, 70-230 mesh particle size; solvent petroleum ether: ethyl acetate 9:1).

(*S*)-4-methyltetrahydro-2H-pyran-2-one: $^1\text{H-NMR}$: (400 MHz, CDCl_3) δ 1.07 (d, $J = 6.3 \text{ Hz}$, 3H), 1.56–1.47 (m, 1H), 1.95–1.89 (m, 1H), 2.15–2.07 (m, 2H), 2.70–2.64 (m, 1H), 4.30–4.23 (m, 1H), 4.44–4.39 (m, 1H).

Isolated (*S*)-4-methyltetrahydro-2H-pyran-2-one contained 0.98% of the lactol intermediate (4-methyltetrahydro-2H-pyran-2-ol), proved by chiral-phase GC analysis.

2.2.8. Photochemical oxidation of NADH

The brand of the LED light source is Paulmann, YourLED, Basic Set RGB 1.5m.



Figure 2.1. Picture of the reaction setup of the photobiocatalytic oxidation reactions

For a total volume of 2 mL reaction, 1950 μL of 50 mM KPi buffer (pH 7), 40 μL of reduced nicotinamide adenine dinucleotide (NADH) (10 mM) and 10 μL of flavin mononucleotide (FMN) (0.4 mM) were added in a Schlenk flask. At intervals, 1 mL samples were withdrawn, analysed spectrophotometrically (Agilent technologies Cary 60 UV-Vis at 25 $^{\circ}\text{C}$) and returned into the reaction mixture.

2.2.9. Biophotocatalytic oxidation of *meso*-3-methyl-1,5-pentanediol

For a total volume of 3 mL reaction, 2100 μL of glycine NaOH buffer (pH 9, 100 mM), 150 μL of *meso*-3-methyl-1,5-pentanediol (200 mM), 300 μL of NADH (10 mM), 150 μL of purified HLADH (148 μM) and 5 drops of catalase were added in a Schlenk flask. A slight overpressure with ambient air was ensured by an air-filled balloon connected to the headspace.

For analysis, 50 μL samples of the reaction mixture were taken at intervals. The extraction of the substrate, the intermediate and the product was performed two times with 125 μL ethyl acetate (containing 5mM acetophenone as internal standard). The separation of the two phases was obtained *via* centrifugation (60 sec). The combined organic phases were dried over anhydrous MgSO_4 and

transferred into GC vials for analysis. All concentrations reported here are based on calibration curves obtained from authentic standards and treated in the same manner as described here.

2.3. Results and discussion

As commercial LEDs come with three individual colours (blue, green and red exhibiting wavelength maxima at 465, 519, and 631 nm respectively, Figure 2.2 A) we investigated each wavelength to promote the photochemical oxidation of NADH.

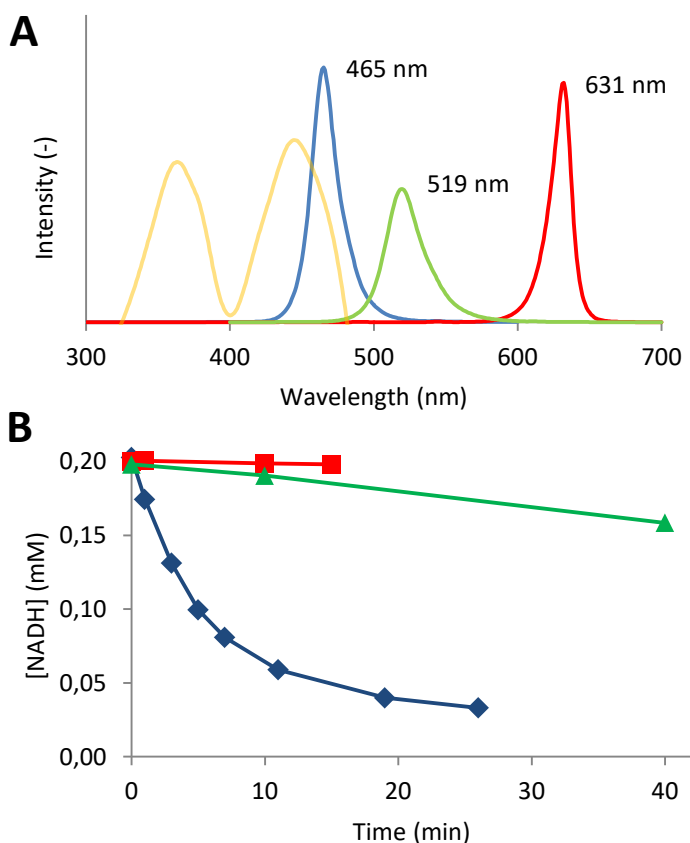


Figure 2.2. Emission wavelengths of the LEDs used (A) and the influence of the LED wavelength on the rate of the photocatalytic aerobic NADH oxidation (B). A: The emission spectra of the blue, green and red LED are shown (in arbitrary units) together with the absorption spectrum of the FMN photocatalyst, yellow. B: Time course of the aerobic oxidation of NADH catalysed by FMN and red (■), green (▲) or blue (◆) light. Conditions: 50 mM KPI buffer (pH 7), $[NADH]_0 = 0.2 \text{ mM}$, $[FMN] = 2 \text{ }\mu\text{M}$, $T = 30 \text{ }^\circ\text{C}$.

In accordance with the mechanism proposed in Scheme 2.1, no conversion of NADH was observed in the absence of either, the photocatalyst, a light source or under anaerobic reaction conditions. As shown in Figure 2.2 B only blue light (λ_{\max} of 465 nm) significantly accelerated the overall reaction while green light (λ_{\max} of 519 nm) yielded significantly lower rate and red light (λ_{\max} of 631 nm) had almost no accelerating influence as compared to 'dark' conditions. In terms of turnover frequencies, the flavin catalysts performed <5, 30 and 680 catalytic cycles per hour under red, green and blue light irradiation, respectively. This trend is in agreement with the relative overlap of the LED emission spectra and the FMN absorption spectrum (Figure 2.2 A). Interestingly, using blue LEDs enabled slightly higher NADH oxidation rates as compared to bright white light bulbs under otherwise identical conditions (Figure 2.3). This observation, however, should not be over-interpreted as a quantitative comparison of the light intensities is yet missing. In terms of light intensity, the LED-based photocatalytic system was well-behaved (Figure 2.4) and the overall rate of the system correlated directly with the intensity of the LED light source.

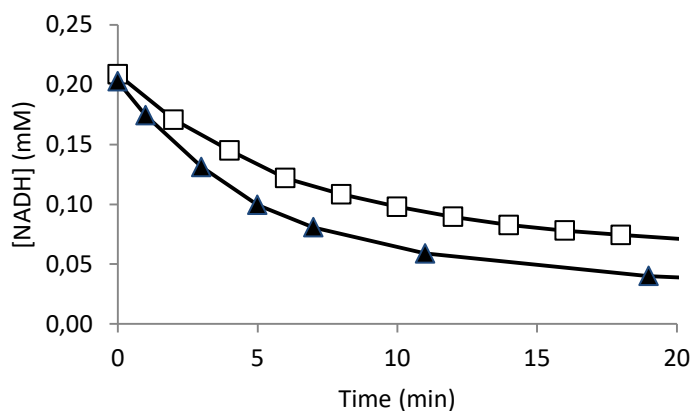


Figure 2.3. Photocatalytic oxidation of NADH using the traditional white light bulb (□) or blue LED light (▲). Conditions: 50 mM KPi buffer (pH 7), $T = 30\text{ }^{\circ}\text{C}$, $[\text{NADH}]_0 = 0.2\text{ mM}$, $[\text{FMN}] = 2\text{ }\mu\text{M}$.

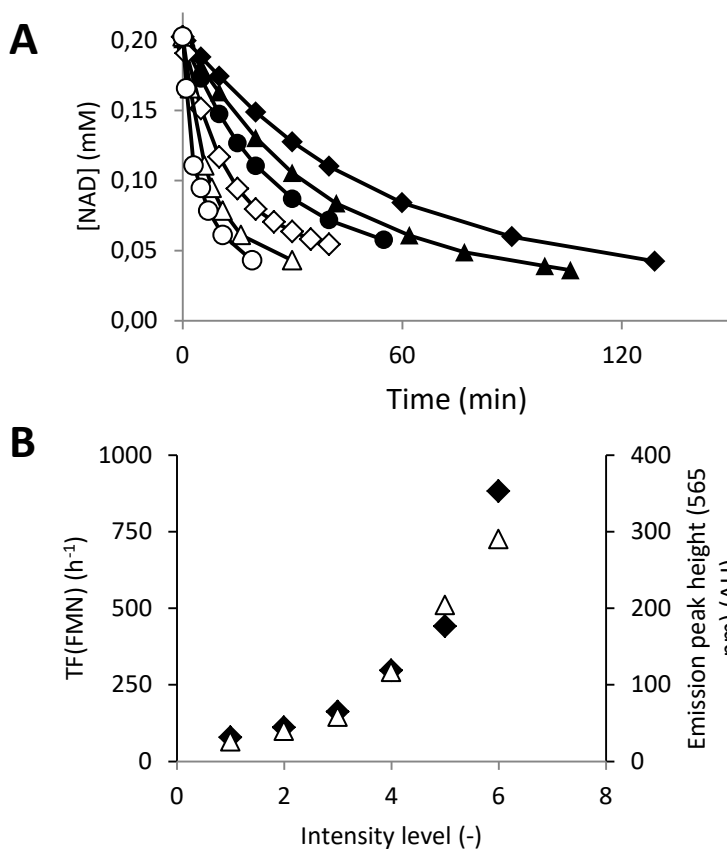


Figure 2.4. A: Influence of the intensity of the blue LED in the oxidation of NADH in presence of FMN. Conditions: 50 mM KPi buffer (pH 7), $T = 30\text{ }^{\circ}\text{C}$, $[\text{NADH}]_0 = 0.2\text{ mM}$, $[\text{FMN}] = 2\text{ }\mu\text{M}$; relative blue light intensity: 1: ◆, 2: ▲, 3: ●, 4: ◇, 5: △, 6: ○; B: dependence of the rate of the FMN-catalysed NADH oxidation (expressed as TF of the FMN catalyst, ◆) on the intensity of the blue LED (△). Conditions: KPi buffer (pH 7, 50 mM), $T = 30\text{ }^{\circ}\text{C}$, $[\text{NADH}]_0 = 0.2\text{ mM}$, $[\text{FMN}] = 2\text{ }\mu\text{M}$.

Another advantage of the LED system is the missing thermal effect on the reaction system as compared to the white light bulb. While with the first no significant temperature change was observed (in the absence of external cooling), the latter lead to a temperature increase of more than $30\text{ }^{\circ}\text{C}$ within one hour under the same conditions (Figure 2.5).

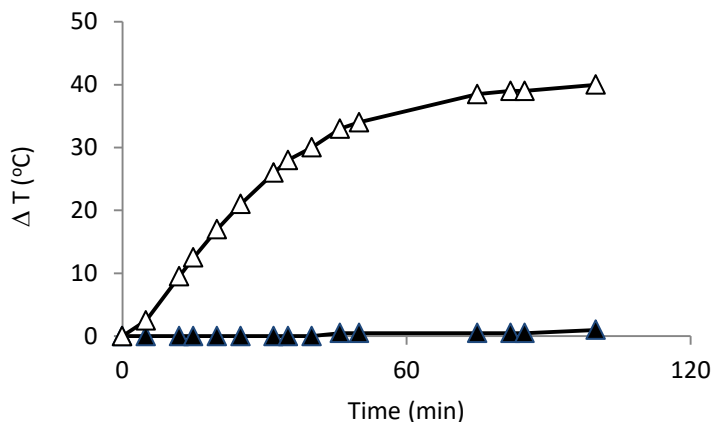
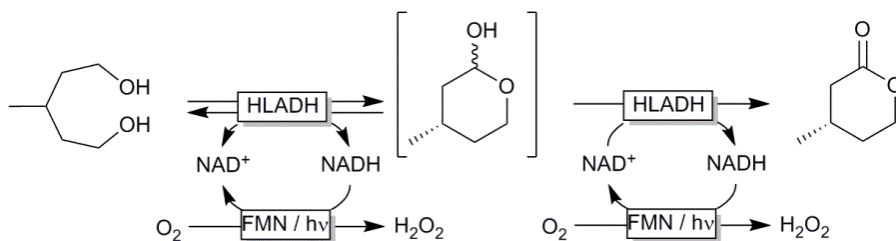


Figure 2.5. Effect of different light sources on the temperature of a non-thermostatted reaction vessel. LEDs (▲) and white light bulb (△).

Encouraged by these results we decided to apply the LED-based photocatalytic NADH oxidation system to the horse liver alcohol dehydrogenase (HLADH) catalysed oxidative lactonisation of α,ω -diols such as *meso*-3-methyl-1,5-pentanediol (Scheme 2.2).²⁰ In this system, HLADH catalyses the enantioselective two-step oxidation of the diol starting material yielding enantiopure (*ee* > 98 %) (*S*)-4-methyltetrahydro-2*H*-pyran-2-one using the oxidised nicotinamide cofactor (NAD^+) as primary hydride acceptor. *In situ* regeneration of NAD^+ from NADH is achieved using the photocatalytic system outlined in Scheme 2.1. Pleasingly, smooth conversion of the starting material into the enantiopure lactone product was observed (Figure 2.6).



Scheme 2.2. Oxidative lactonisation of *meso*-3-methyl-1,5-pentanediol to (*S*)-4-methyltetrahydro-2*H*-pyran-2-one using horse liver alcohol dehydrogenase (HLADH) and photocatalytic, aerobic regeneration of NAD^+ .

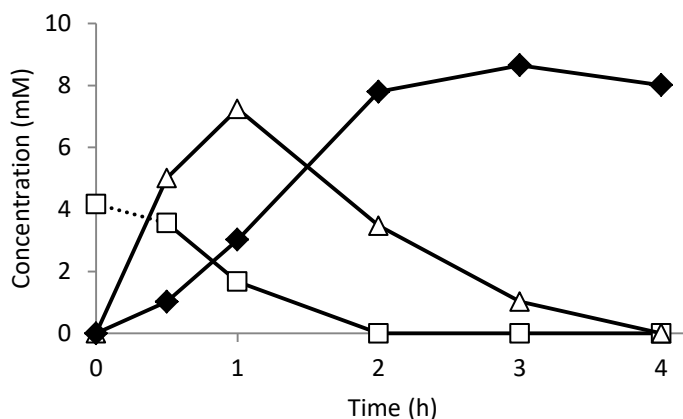


Figure 2.6. Time course of the photoenzymatic oxidation of meso-3-methyl-1,5-pentanediol to (S)-4-methyltetrahydro-2H-pyran-2-one via the intermediate lactol. General conditions: 100 mM glycine-NaOH buffer pH 9 100 mM, $[diol]_0 = 10$ mM, $[NADH]_0 = 1$ mM, $[FMN] = 100$ μ M, $[HLADH] = 7.4$ μ M, 5 drops of catalase, $T = 30$ $^{\circ}$ C.

Within the first 2 hours of the reaction the mass balance of the reaction was closed (sum of all reagents 10 ± 0.2 mM) and decreased to 8 mM after 4 hours. This observation is explained by the slow, spontaneous hydrolysis of the lactone to the corresponding hydroxy acid.¹⁷ This finding is also supported by the significant acidification of the reaction mixture at higher substrate loading (Figure 2.7). Further optimisations to minimise or prevent this undesired side reaction are currently underway. For example, a tighter pH control and *in situ* extraction of the lactone product are promising approaches to circumvent the undesired hydrolysis.

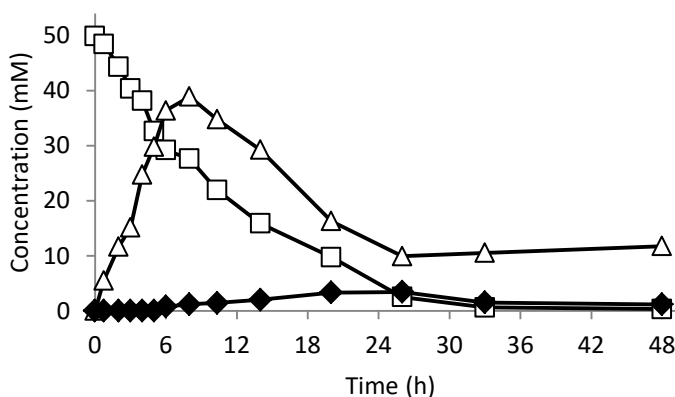


Figure 2.7. Time course of the photoenzymatic oxidation of meso-3-methyl-1,5-pentanediol (\square) to (S)-4-methyltetrahydro-2H-pyran-2-one (\blacklozenge) via the intermediate lactol (\triangle). General conditions: 200 mM glycine-NaOH buffer (pH 9.5), $[diol]_0 = 50$ mM, $[NADH]_0 = 1$ mM, $[FMN] = 100$ μ M, $[HLADH] = 7.4$ μ M, 5 drops of catalase, $T = 30$ $^{\circ}$ C.

The catalytic activity of the photocatalyst was 122 h^{-1} and thereby significantly lower than determined before (Figure 2.4). Partially this can be attributed to the higher pH value of the reaction medium.¹¹ To assess the environmental impact of the presented photobiocatalytic oxidative lactonisation, we performed an E-factor analysis (Table 2.1).^{21,22}

Table 2.1. Estimation of the wastes generated in the photobiocatalytic lactonisation reactions

Contribution	White light bulb	LED
Water		877
Buffer (glycine)		6.6
NAD		0.6
FMN		0.04
HLADH		0.25
Ethyl acetate ^a		1973
CO ₂ from cooling ^b	40.4	0
CO ₂ from light source ^b	40 780	3920

^aUsed as extraction solvent for GC analysis. ^bTo estimate the CO₂ emissions due to electricity consumption, we used the average European CO₂ emission intensity.

Though shocking at first sight, these numbers also guide us to optimise the proposed photobiocatalytic reaction system *en route* to higher sustainability. First of all, the overall substrate loading (and the resulting product titres, respectively) must be increased significantly. In these experiments, 10 mM product accumulated resulting in an enormous amount of waste water. This is obviously unacceptable, both from an environmental and an economical point-of-view. Raising the product titres to industrially demanded 50-200 g.L⁻¹ will reduce the E-factor to approx. 5-20. Similarly, also the contributions of buffers and catalysts will be reduced. The very high E-factor contribution of the extraction solvent should not be taken too serious, the aim of the extraction procedure was to adequately determine the reagent concentrations and not to establish an environmentally friendly downstream processing (DSP) method. Nevertheless, the high solvent consumption again exemplifies the importance of DSP to the overall environmental impact.²³ Finally, we made an attempt to quantify the 'hidden E-factor' contributions caused by the electrical power consumed. The calculation of the CO₂ emissions was straightforward using the power consumptions provided by the manufacturers.

Again, the exorbitant values shown in Table 2.1 should not be taken too seriously as relatively large light sources were used for a rather small reaction volume. Raising the product concentration together with increasing the reaction volume can easily reduce the E-factor by several orders of magnitude to acceptable values. These experiments are currently underway. Nevertheless, Table 2.1 also visualises the significant positive contribution that LED technology can have on the sustainability of photo(bio)catalytic reactions!

The energy consumption caused by heating (or cooling) of the reaction mixture is usually not included in E-factor calculations. Table 2.1, however, demonstrated that this 'hidden contribution' by no means is to be neglected as it easily exceeds the contributions of the reagents.

Overall, the use of simple LEDs represents a simple, more user-friendly alternative compared to bright white light bulbs. More excitingly, LEDs also offer significant advantages in terms of energy efficiency as futile wavelengths and heat generation are omitted. Taking together the lower power consumption with the increased catalytic activity of the LED system a more than 90% decrease of energy consumption (and corresponding CO₂ emissions) can be achieved. Furthermore, the significant thermal effect of the white light bulb also necessitates additional cooling of the reaction mixture, which can be reduced or even omitted in case of the LEDs.

2.4. Conclusions

Nowadays, photocatalysis is in focus of catalysis research.²⁴⁻²⁶ Comparably few studies deal with photocatalysis to promote biocatalytic reactions, a 'combination of two intrinsically green technologies'.²⁷

However, neither biocatalysis nor photocatalysis are environmentally sustainable *per se*. A (self-)critical evaluation of the possible environmental impact is necessary to substantiate 'green claims' and to identify bottlenecks as a basis for improved reaction setups *en route* to truly sustainable procedures.

In this study, we have demonstrated that simple LEDs are well-suited to substitute conventional light sources in flavin-based NAD⁺ regeneration systems to promote dehydrogenase-catalysed oxidation reactions. Particularly, the significantly decreased energy demand of LED systems makes it attractive envisioning environmentally acceptable syntheses.

2.5. References

1. *Enzyme Catalysis in Organic Synthesis*, ed. K. Drauz, H. Groeger and O. May, Wiley-VCH, Weinheim, 2012.
2. K. Faber, *Biotransformations in Organic Chemistry*, Springer, Berlin, 6th ed., 2011.
3. F. Hollmann, I. W. C. E. Arends, K. Buehler, A. Schallmeyer and B. Buhler, *Green Chem.*, 2011, **13**, 226-265.
4. W. Kroutil, H. Mang, K. Edegger and K. Faber, *Curr. Opin. Chem. Biol.*, 2004, **8**, 120-126.
5. S. Kara, J. H. Schrittwieser, F. Hollmann and M. B. Ansorge-Schumacher, *Appl. Microbiol. Biotechnol.*, 2014, **98**, 1517–1529.
6. C. Holec, K. Neufeld and J. Pietruszka, *Adv. Synth. Catal.*, 2016, **358**, 1810-1819.
7. B. R. Riebel, P. R. Gibbs, W. B. Wellborn and A. S. Bommarius, *Adv. Synth. Catal.*, 2002, **344**, 1156-1168.
8. R. Jiang and A. S. Bommarius, *Tetrahedron Asymm.*, 2004, **15**, 2939-2944.
9. J. T. Park, J.-I. Hirano, V. Thangavel, B. R. Riebel and A. S. Bommarius, *J. Mol. Catal. B: Enzym.*, 2011, **71**, 159-165.
10. S. Aksu, I. W. C. E. Arends and F. Hollmann, *Adv. Synth. Catal.*, 2009, **351**, 1211-1216.
11. S. Gargiulo, I. W. C. E. Arends and F. Hollmann, *ChemCatChem*, 2011, **3**, 338-342.
12. S. Kochius, Y. Ni, S. Kara, S. Gargiulo, J. Schrader, D. Holtmann and F. Hollmann, *ChemPlusChem*, 2014, **79**, 1554-1557.
13. J. B. Jones and K. E. Taylor, *J. Chem. Soc., Chem. Commun.*, 1973, 205 - 206.
14. V. Massey, *J. Biol. Chem.*, 1994, **269**, 22459-22462.
15. D. Holtmann and F. Hollmann, *ChemBioChem*, 2016, **17**, 1391-1398.
16. M. De La Rosa, J. Navarro and M. Roncel, *Appl. Biochem. Biotechnol.*, 1991, **30**, 61-81.
17. C. T. Chung, S. L. Niemela, R. H. Miller, *Proc. Natl. Acad. Sci. U. S. A.*, 1989, **86**, 2172–2175.
18. D. J. Philipps, A. E. Graham, *Synlett* 2008, **5**, 649.
19. S. Kara, D. Spickermann, J. H. Schrittwieser, A. Weckbecker, C. Leggewie, I. W. C. E. Arends, F. Hollmann, *ACS Catalysis*, 2013, **3** (11), 2436-2439.
20. S. Kara, D. Spickermann, J. H. Schrittwieser, A. Weckbecker, C. Leggewie, I. W. C. E. Arends and F. Hollmann, *ACS Catalysis*, 2013, **3**, 2436-2439.

21. R. A. Sheldon, *Chem. Commun.*, 2008, 3352-3365.
22. Y. Ni, D. Holtmann and F. Hollmann, *ChemCatChem*, 2014, **6**, 930-943.
23. J. Schrittwieser, F. Coccia, S. Kara, B. Grischek, W. Kroutil, N. d'Alessandro and F. Hollmann, *Green Chem.*, 2013, **15**, 3318-3331.
24. R. Brimiouille, D. Lenhart, M. M. Maturi and T. Bach, *Angew. Chem. Int. Ed.*, 2015, **54**, 3872-3890.
25. K. L. Skubi, T. R. Blum and T. P. Yoon, *Chem. Rev.*, 2016, **116**, 10035-10074.
26. R. N. Perutz and B. Procacci, *Chem. Rev.*, 2016, **116**, 8506-8544.
27. J. A. Maciá-Agulló, A. Corma and H. Garcia, *Chem. Eur. J.*, 2015, **21**, 10940-10959.

Chapter 3:

Photochemical regeneration of flavoenzymes – an Old Yellow Enzyme case-study

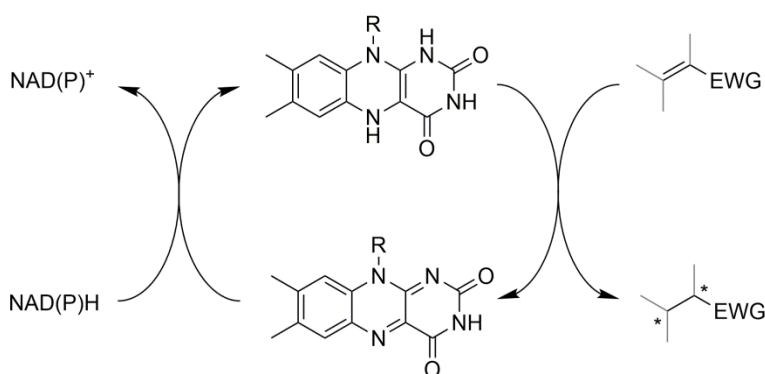
Direct, NAD(P)H-independent regeneration of old yellow enzymes represents an interesting approach for simplified reaction schemes for the stereoselective reduction of conjugated C=C-double bonds. Simply by illuminating the reaction mixtures with blue light in the presence of sacrificial electron donors enables to circumvent the costly and unstable nicotinamide cofactors and a corresponding regeneration system. In the present study, we characterise the parameters determining the efficiency of this approach and outline the current limitations. Particularly, the photolability of the flavin photocatalyst and the (flavin-containing) biocatalyst represent the major limitation *en route* to preparative application.

This chapter is based on

M.C.R. Rauch, M. Pesic, M.M.E. Huijbers, M. Pabst, C.E. Paul, I.W.C.E. Arends, F. Hollmann, *BBA – Proteins Proteomics*, 2020, **1868**, 140303.

3.1. Introduction

Ene-reductases from the Old Yellow Enzymes (OYEs) family have been known for close to a century.¹ They catalyse the stereospecific *trans*-hydrogenation of conjugated C=C-double bonds creating up to two new chiral centres (Scheme 3.1).



Scheme 3.1. Reduction of activated C=C-double bonds by Old Yellow Enzymes (OYEs). EWG = electron withdrawing group (typically a carbonyl group).

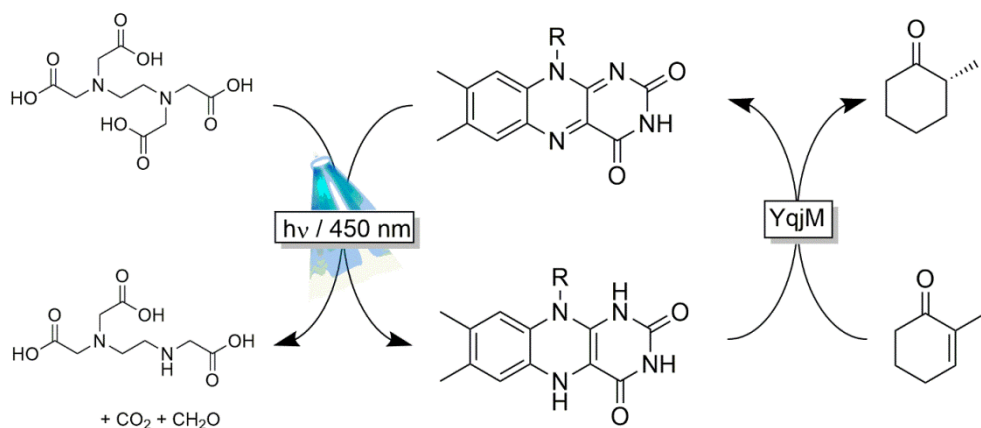
Their potential as catalysts for organic synthesis, however, has only been recognised by Faber, Hauer and coworkers a decade ago.^{2,3} Ever since then, preparative applications of OYEs are increasing exponentially^{4,5} with the first examples of industrial application.^{6,7}

OYEs contain a flavin prosthetic group – mostly a flavin mononucleotide (FMN) – which in the first half-reduction reaction of the catalytic mechanism is reduced by the nicotinamide adenine dinucleotide cofactor (NAD(P)H). In the second half-oxidation reaction of the mechanism, the reduced flavin transfers a hydride ion in a Michael-type addition to the β -carbon atom of the enzyme-bound unsaturated substrate followed by protonation of the resulting enolate anion in a *trans* fashion.

In the past years, a range of alternative reductants have been reported replacing the costly and unstable nicotinamide cofactors.⁸ Amongst them, chemical reductants such as synthetic nicotinamides⁹⁻¹² or transition metal catalysts^{13,14} have been proposed. Also photochemical approaches are gaining attention.¹⁵⁻²⁶ The latter approaches mostly utilise FMN (the prosthetic group of OYEs) as

photocatalyst to channel electrons from a sacrificial electron donor (e.g. EDTA) to the OYE's active site (Scheme 3.2). The photochemistry of the (yellow) flavin photocatalyst has been established decades ago,²⁷⁻³¹ but a critical evaluation of their practical usefulness is so far missing. We therefore set out to investigate the scope and limitations of direct, photochemical regeneration of FMN to promote OYE-catalysed reduction reactions.

As a model reaction for our investigations, we chose the stereospecific reduction of 2-methylcyclohexenone to (*R*)-2-methylcyclohexanone catalysed by the OYE homologue from *Bacillus subtilis* (YqjM) (Scheme 3.2).³²⁻³⁴



Scheme 3.2. Photoenzymatic reduction of 2-methylcyclohexenone to (*R*)-2-methylcyclohexanone using YqjM as biocatalyst. In situ regeneration of the reduced flavin prosthetic group is achieved using photoexcited FMN in the presence of EDTA as sacrificial electron donor.

3.2. Material and methods

3.2.1. Chemicals

Unless stated otherwise all chemicals were purchased from Sigma-Aldrich (Steinheim, Germany), New England Biolabs (Ipswich, MA, USA) or Merck (Darmstadt, Germany) in the highest quality available and used without further purification.

3.2.2. Analytics

Gas chromatography (GC) analysis:

GC measurements were performed on a Shimadzu GC-14A equipped with a CP-Chirasil Dex CB (25 m x 0.32 mm x 0.25 μ m, Macherey & Nagel, Düren, Germany) and flame-ionization detection (FID).

The Size Exclusion Chromatography column is Superdex 200 Increase 10/300 GL on a NGC Chromatography System from Biorad with a loop of 200 μ L. The flow rate was 10 mL/min of a KPi buffer 100 mM pH 6.5 + 150 mM KCl.

For circular dichroism, the instrument used is a Jasco J-815 CD Spectrometer with the Jasco PFD-425S/15 temperature controller. The spectroscopic analysis were recorded from 260 to 190 nm with data pitch of 0.5 nm, continuous scanning mode, scanning speed of 100 nm/min, response of 0.5, band width of 1 nm and accumulation of 20.

3.2.3. Bacterial strains and plasmids

The plasmid pET28a containing the gene encoding the Old Yellow Enzyme from *Bacillus subtilis* (YqjM) bearing an additional N-terminal His₆-tag was transformed into the appropriate *E. coli* BL21 (DE3).³⁵

3.2.4. Cultivation conditions

Expression of YqjM was carried out by inoculation of 1 L of autoinduction ZYM-5052 media³⁶ supplied with the appropriate antibiotic (kanamycin) with an overnight culture. Cells were grown overnight at 37 °C in baffled shake flasks. Cells were harvested (centrifugation at 10000 *g* at 4 °C for 15 min) and washed twice in potassium phosphate buffer (pH 6.5, 20 mM). The bacterial cell pellet was resuspended in the same buffer. Mechanical cell disruption was effected by using Multi Shot Cell Disruption System (Constant Systems). Cell debris were separated from the crude extract by centrifugation.

3.2.5. Purification of YqjM

The supernatant was loaded to 14 mL Nickel-NTA column (GE Healthcare, Munich, Germany). After washing the column with a triple volume of 20 mM sodium phosphate buffer containing 30 mM imidazole pH 6.5, the protein was eluted with 20 mM potassium phosphate buffer containing 250 mM imidazole pH 6.5. Fractions containing proteins were tested with UV assay and those containing YqjM were collected and incubated with 5 mM of FMN. After 30 min of incubation on ice, enzyme suspension was desalted twice using PD-10 columns in order to remove the excess of FMN and concentrated using Amicon (30 kDa cut-off).

3.2.6. Determination of YqjM activity

The YqjM activity assay was established with 2-methylcyclohex-2-en-1-one as standard substrate. The consumption of NADPH during the enzymatic reaction was directly followed at 340 nm for 120 s. The 2-methylcyclohex-2-en-1-one concentration in the assay was 1 mM and the initial concentration of NADPH was 150 μ M. Because of background activity with oxygen, glucose and glucose oxidase was also added at a concentration of 20 mM and 10 U/mL respectively. The buffer used was KPi buffer 100 mM pH 6.5.

In order to calculate the half-life time of YqjM under different conditions, residual activity was determined over time. The curves were fitted with an exponential regression in Excel and from the value of the exponential equation, the half-life time was calculated.

3.2.7. Determination of Formate Dehydrogenase (FDH) activity

The FDH activity assay was established with formate as standard substrate. The formation of NADH during the enzymatic reaction was directly followed at 340 nm for 120 s. Formate concentration in the assay was 75 mM and the initial concentration of NAD⁺ was 250 μ M. The buffer used was KPi buffer 50 mM pH 7.

3.2.8. Determination of ADH-A activity

The ADH-A activity assay was established with isopropanol as standard substrate. The formation of NADH during the enzymatic reaction was directly followed at 340 nm for 120 s. isopropanol concentration in the assay was 500 mM and the initial concentration of NAD⁺ was 400 μ M. The buffer used was Tris buffer 50 mM pH 8.

3.2.9. Determination of OYE2 activity

The OYE2 activity assay was established with 2-methylcyclohex-2-en-1-one as standard substrate. The consumption of NADPH during the enzymatic reaction was directly followed at 340 nm for 120 s. The 2-methylcyclohex-2-en-1-one concentration in the assay was 1 mM and the initial concentration of NADPH was 150 μ M. Because of background activity with oxygen, glucose and glucose oxidase was also added at a concentration of 20 mM and 10 U/mL respectively. The buffer used was KPi buffer 100 mM pH 6.5.

3.2.10. Determination of 3-hydroxybenzoate-6-hydroxylase (3HB6H) activity

The 3HB6H activity assay was established with 3-hydroxybenzoic acid as standard substrate. The consumption of NADH during the enzymatic reaction was directly followed at 340 nm for 120 s. The 3-hydroxybenzoic acid concentration in the assay was 5 mM and the initial concentration of NADH was 150 μ M. The buffer used was Tris-H₂SO₄ 50 mM pH 8.

3.2.11. Trypsin digestion and MS analysis

Samples of illuminated and native YqjM were prepared by incubation in SDS-PAGE loading buffer at 40 °C for 5 min. Samples were loaded and analysed on 10% polyacrylamide gels (precast gel, BioRad, Cat No 4568034). Following staining using Coomassie Blue, bands were cut, gel pieces were destained, proteins were reduced using DTT and carbamidomethylated using IAA. Proteins were digested in-gel using Trypsin at 37 °C overnight, extracted and speed vac dried. The resuspended samples (3% acetonitrile in H₂O, 0.1% formic acid) were

analysed by tandem mass spectrometry using M-Class HPLC system online coupled to ESI-Q-TOF premier (Waters, UK).

An aliquot of approximately 0.3 μg protein was injected to the LC-MS analysis system, operating in DDA mode. Data were analysed using MassLynx 4.1 and PEAKS Studio for sequence coverage and abundant residue modifications such as oxidation.

3.2.12. Photobiocatalytic reduction of 2-methylcyclohex-2-en-1-one by YqjM

For each reaction, all chemicals were added first in a glass reaction vessel, except the enzyme and the substrate. Then, the reaction was degassed with N_2 during 30 min and finally, before switching on the light, the enzyme and the substrate were added anaerobically to the reaction with a needle. A slight overpressure with N_2 gas was ensured by two N_2 -filled balloons (one with a long needle to take samples and the second one with a short needle to keep an overpressure while taking samples) connected to the headspace.



Figure 3.1. Picture of the setup

For analysis, 125 μL samples of the reaction mixture were taken at intervals. The extraction of the substrate and the product was performed two times with 125 μL of ethyl acetate (containing 5 mM of dodecane as internal standard). The separation

of the two phases was obtained *via* centrifugation. The combined organic phases were dried over anhydrous MgSO_4 and transferred into a GC vials for analysis.

All concentrations reported on this paper are based on calibration curves obtained from authentic standards and treated in the same manner as described here. The enantiomeric excess (*ee*) value during this study was >90%, knowing that the substrate is only pure at 90% (the 10% of impurity is a racemic mixture of 6-methylcyclohex-2-en-1-one which can also be reduced by YqjM).

3.3. Results and discussion

Recombinant YqjM was produced in *Escherichia coli* using an autoinduction medium.³⁵⁻³⁷ His-Tag containing YqjM was purified by affinity chromatography using Ni-NTA chromatography column.

For the photochemical reaction outlined in Scheme , we used commercial LEDs ($\lambda=450$ nm) as light source wrapped around the reaction vessel (Figure 3.1). With this setup, full conversion of 10 mM 2-methylcyclohexenone could be achieved within less than 5h (Figure 3.2). No further side product was observed using gas chromatography for analysis.

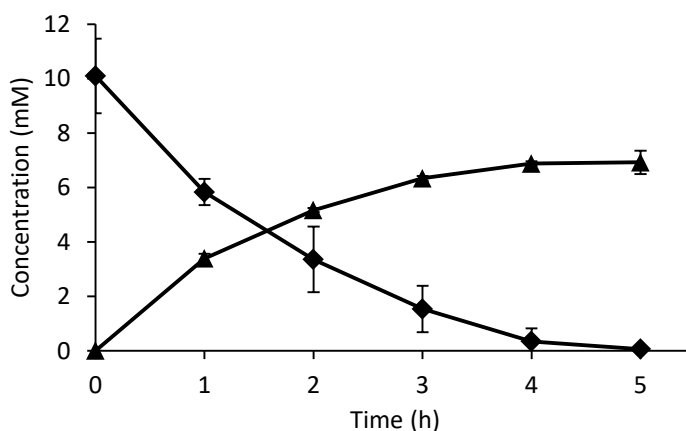


Figure 3.2. Time-course of the photoenzymatic reduction of 2-methylcyclohex-2-en-1-one (◆) to (R)-2-methylcyclohexanone (▲). Conditions: 100 mM potassium phosphate buffer (pH 6.5), [2-methylcyclohex-2-en-1-one] = 10 mM; [FMN] = 0.2 mM, [YqjM] = 6.9 μM , [EDTA] = 50 mM, $T = 30$ °C, light source: blue LED (450 nm, 80 $\mu\text{W}\cdot\text{cm}^{-2}$). During the reaction, anaerobic conditions were maintained leading a N_2 stream over the reaction.

The enantioselectivity of the reaction was superb ($ee >99.5\%$) as throughout the experiment only traces of the (*S*)-enantiomer were observed. This finding also confirms our assumption of the enzymatic reduction of the conjugated C=C-double bond as the direct reduction by the reduced mediator would have yielded racemic product. It is worth mentioning that anaerobic reaction conditions were essential for the reaction as in the presence of molecular oxygen, lower reaction rates were observed ($2.04 \text{ mM}\cdot\text{h}^{-1}$ instead of $3.39 \text{ mM}\cdot\text{h}^{-1}$). This is in line with some previous findings about the high reactivity of reduced flavins in the presence of O_2 .³⁸⁻⁴³ Therefore, we applied a gentle N_2 stream over the reaction mixture to maintain anaerobic reaction conditions. This, however, also led to some increased evaporation of the reagents (as confirmed in appropriate control experiments), explaining the rather poor mass balance of approximately 70%. Improved reaction setups including condensers to minimise the reagent evaporation will circumvent this technical issue.

The catalytic performance of YqjM in terms of turnover frequency (TF = amount of product formed in time divided by the amount of YqjM used) was only in the range of 8 min^{-1} and thereby fell back significantly behind the activities reported using NADPH as reductant.³² We therefore decided to investigate the parameters influencing the reaction rate in more detail. Particularly, we systematically varied the concentration of the photocatalyst (Figure 3.3 A), the biocatalysts (Figure 3.3 B), the light intensity (Figure 3.3 C) and the concentration of the sacrificial reductant (Figure 3.3 D).

Varying the photocatalyst concentration, we observed a saturation-type behaviour of the reaction rate with increasing FMN concentrations. Half-maximal reaction rates were observed at FMN concentration around $200 \mu\text{M}$. This is almost 100-fold higher than the K_M value determined for the natural reductant (NADPH)³⁴ suggesting that the interaction of the (reduced) FMN to the active site of YqjM may be overall rate-limiting due to the sterically impaired interaction and sub-optimal electron transfer from the photocatalytic FMN to the enzyme-bound FMN.

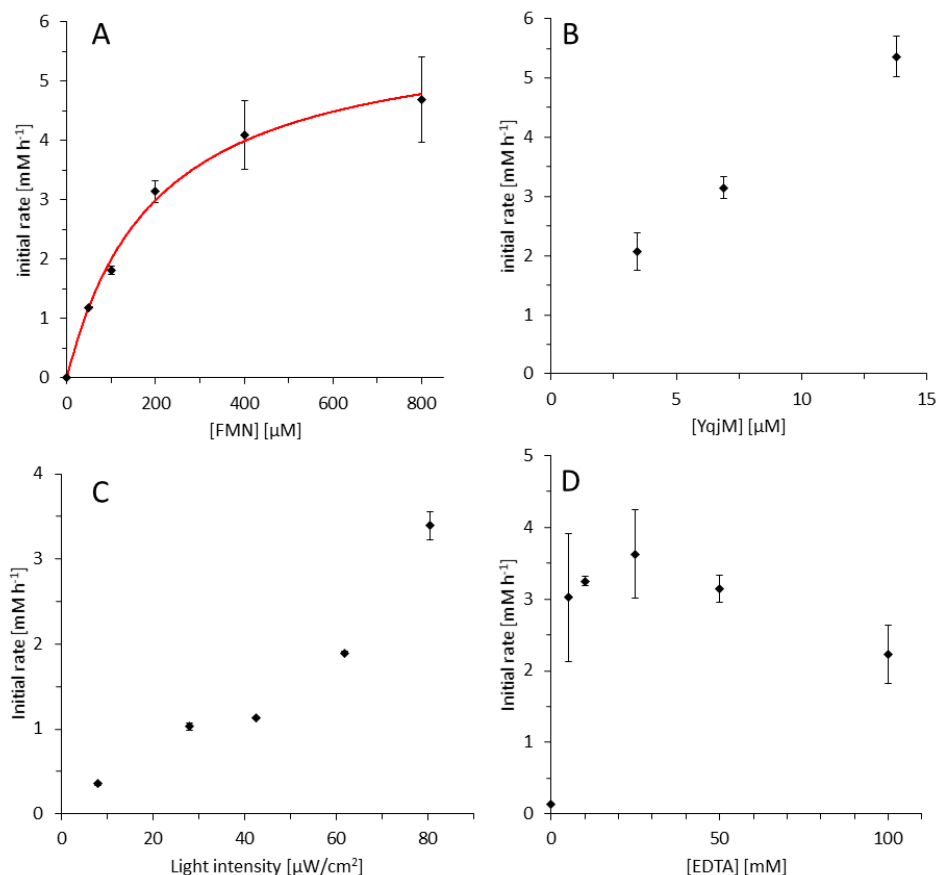


Figure 3.3. Influence of the photocatalyst concentration (A), the enzyme concentration (B), the light intensity (C) and the sacrificial electron donor concentration (D) on the reduction rate of 2-methylcyclohexenone. Unless stated in the graph the following conditions were used: 100 mM potassium phosphate buffer (pH 6.5), [2-methyl cyclohexenone] = 10 mM; [FMN] = 0.2 mM, [YqjM] = 6.9 μM, [EDTA] = 50 mM, T = 30 °C, light source: blue LED (450 nm, 80 μW.cm⁻²). During the reaction, anaerobic conditions were maintained leading a N₂ stream over the reaction.

Increasing the biocatalyst concentration resulted in an almost linear increase of the overall reaction rate, which is in-line with the assumption of the reduction of YqjM being overall rate-limiting. The same is true for the observed influence of the light intensity. Higher photon fluxes are expected to yield higher concentrations of photoexcited flavins and therewith increase the concentration of reduced external flavins. Interestingly enough, the concentration of the sacrificial electron donor (EDTA) had only a minor influence on the overall rate. Only marginal conversion

was observed in the absence of EDTA, which may be explained by the photochemical reduction of FMN by traces of 'contaminating' reductants (vide infra). Between an EDTA concentration of 5 to 50 mM, the overall rate remained largely unchanged and slightly decreased at higher EDTA concentrations. Interestingly enough, activity assays of YqjM in the presence of elevated EDTA concentrations gave no indication for an inhibitory effect of EDTA (e.g. by removal of structurally relevant metal cations). Hence, at present stage we are lacking a plausible explanation for the decreased productivity of the photocatalytic system at higher EDTA concentrations.

Encouraged by these results we aimed at scaling up the reaction by increasing the substrate concentration to 50 mM. Unfortunately, product accumulation ceased after approximately 5 h (Figure 3.4 A), which interestingly was also the time span of the experiment shown in Figure 3.2. We ascribe this observation to a poor stability of YqjM under the reaction conditions. Indeed, product formation resumed upon addition of fresh biocatalyst (Figure 3.4 B) resulting in the accumulation of 36 mM of enantiopure product (72% yield and 100% conversion due to the above-mentioned evaporation issue). YqjM performed more than 2500 catalytic cycles in this experiment.

Therefore, we investigated the stability of YqjM under different conditions (Figure 3.5). If incubated in buffer in the presence of FMN but in the dark, YqjM was relatively stable with a half-life time of approximately 33 h. This value, however, dramatically dropped upon illumination with blue light (both in the presence and absence of external FMN) and the apparent half-life time of YqjM dropped to less than 2 h. Interestingly, under reducing conditions, i.e. in the presence of EDTA (or NADH), this decrease was somewhat less pronounced ($t_{1/2} \approx 5.5$ h). Furthermore, illumination with either red or green light had a far less detrimental effect on the stability of YqjM.

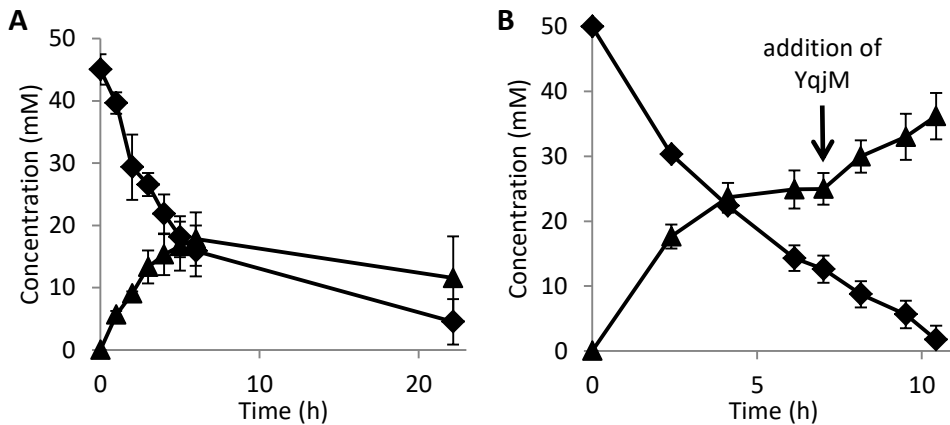


Figure 3.4. Time-course of the photoenzymatic reduction of 2-methylcyclohex-2-en-1-one (◆) to (R)-2-methylcyclohexanone (▲) (A) without or (B) with addition of 6.9 μM of fresh YqjM. Conditions: 100 mM potassium phosphate buffer (pH 6.5), [2-methylcyclohex-2-en-1-one] = 50 mM; [FMN] = 0.2 mM, [YqjM] = 6.9 μM , [EDTA] = 50 mM, $T = 30^\circ\text{C}$, light source: blue LED (450 nm, 80 $\mu\text{W}\cdot\text{cm}^{-2}$). During the reaction, anaerobic conditions were maintained leading a N_2 stream over the reaction.

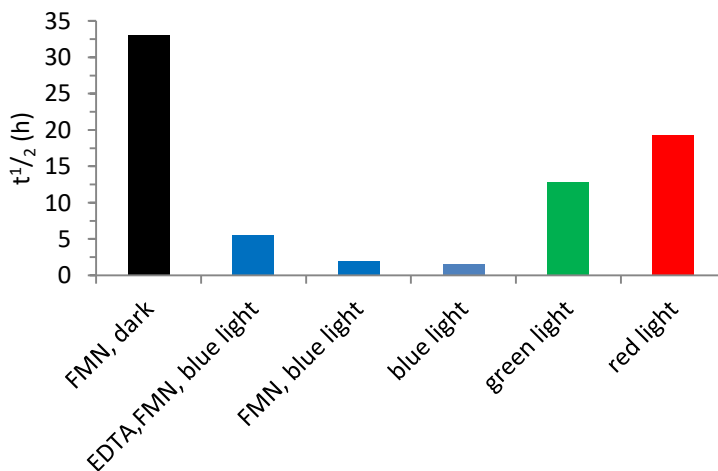


Figure 3.5. Stability of YqjM under different incubation conditions. Conditions: 6.88 μM of YqjM in KPi buffer 100 mM pH 6.5 in presence of either 200 μM of FMN and/or 50 mM of EDTA and illuminated by either blue, red or green LED or protected from any light source, $T = 30^\circ\text{C}$. Activity assay conditions: 20 mM of glucose, 150 μM of NADPH, 10 U/mL of glucose oxidase, 1 mM of 2-methylcyclohex-2-en-1-one and 0.85 μM of YqjM.

These results are most straight-forward explained by photodegradation of the enzyme-bound FMN.⁴⁴⁻⁴⁷ Under dark conditions, virtually none of the YqjM-tightly bound FMN is photoexcited and therefore stable. The emission spectra of the green and red LEDs used in this experiment hardly overlap with the FMN

absorption spectrum⁴¹ and therefore only lead to minor photoexcitation and photodegradation on YqjM-tightly bound FMN (green light overlaps somewhat more and therefore also decreases the half-life time of YqjM more pronouncedly). The effect of the reducing conditions may be explained by the significantly reduced absorption of reduced flavins at 450 nm. This assumption is also supported by the spectral changes recorded for both YqjM and free FMN upon illumination with blue light (Figure 3.6).

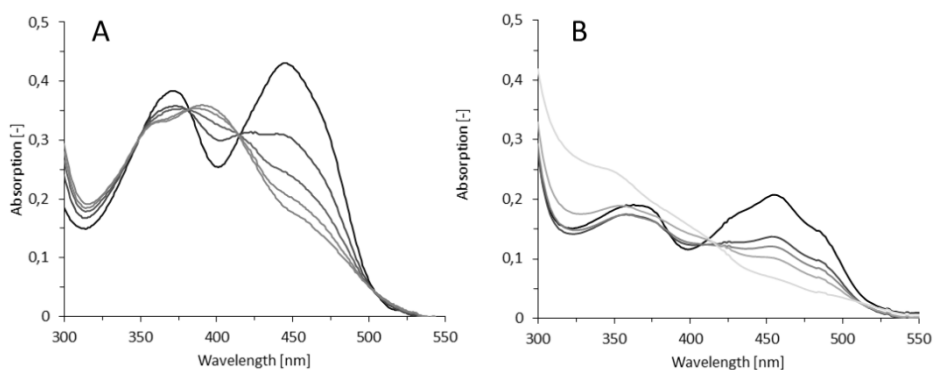


Figure 3.6. Spectral changes observed for FMN (A) and YqjM (B) upon illumination with blue light. FMN (A): spectra were taken at 0, 1, 2, 4 and 8 min (from dark to light); YqjM (B): spectra were taken 0, 1, 2, 5 and 23 h (from dark to light). General conditions: 20 μM of YqjM or FMN in KPi buffer 100 mM pH 6.5 illuminated by blue LED, 80 $\mu\text{W}\cdot\text{cm}^{-2}$, $T = 30^\circ\text{C}$.

For a further validation of the hypothesised photodegradation of enzyme-bound flavin, we also illuminated some enzymes with blue light and determined their residual activity (Table 3.1). For this, two flavin-dependent enzymes and two enzymes not containing a flavin prosthetic group were incubated in the presence and absence of blue light.

Table 3.1. Residual activity of some biocatalysts in the presence of blue light.

Enzyme	Contains flavin	Half-life time in the dark [h]	Half-life time under illumination [h]	Half-life time decrease due to illumination [%]
ADH-A ^[a]	No	8.5	7.4	13
CbFDH ^[b]	No	6.5	4.0	38
3HB6H ^[c]	Yes	0.3	0.1	60
ScOYE2 ^[d]	Yes	10.7	3.7	65

[a] Alcohol dehydrogenase from *Rhodococcus ruber* DSM 44521^{48, 49} [b] Formate dehydrogenase from *Candida boidinii*⁵⁰⁻⁵² [c] 3-Hydroxybenzoate-6-hydroxylase from *Rhodococcus jostii* RHA1⁵³⁻⁵⁵ [d] OYE2 from *Saccharomyces cerevisiae*.^{56, 57}

Hence, photochemical degradation of both, the enzyme-bound FMN and the external (photocatalytic) FMN can be assigned as the major factors limiting the robustness of the photoenzymatic reduction of conjugated C=C-double bonds.

Still, in the course of our experiments we also frequently observed a precipitate, which we believed to be denatured YqjM. SDS-PAGE gel analysis revealed a loss of soluble protein under blue light illumination. Furthermore, circular dichroism analysis of the illuminated enzyme pointed towards some loss in the integrity of the tertiary structure of the enzyme. Size exclusion chromatography of a light treated sample of YqjM showed an aggregation of enzymes overtime. We also performed a proteolytic digest of the illuminated and native YqjM using trypsin and analysed the resulting peptides by mass spectrometry for degradation products. This revealed that in the illuminated YqjM, two methionine residues (M14 and M134) were oxidised to the corresponding sulfoxides (Figure 3.7). Although some oxidation of another methionine was observed already for the non-illuminated protein, the degree of sulfoxidation increased very significantly after exposure to light. Interestingly enough, illumination of the YqjM samples occurred under anaerobic conditions (using a stream of N₂ gas) which makes H₂O₂ a rather unlikely oxidant for this reaction. Possibly, photoexcited flavins can directly oxidise methionine *via* a so far unknown mechanism and electron sink. It is also worth mentioning that this analysis did not cover the entire YqjM polypeptide, therefore, at present time we cannot exclude further modifications of the protein to account for the decreasing stability under illumination. As these amino acids are at the surface of the protein, oxidation of these amino acids may well account for the protein aggregation and precipitation observed. Similar effects have been already

described for oxidative stress related biological aging and degradation.⁵⁸ Future experiments with YqjM mutants devoid these methionine residues will show if such mutants exhibit higher robustness under the photochemical reaction conditions.⁵⁹

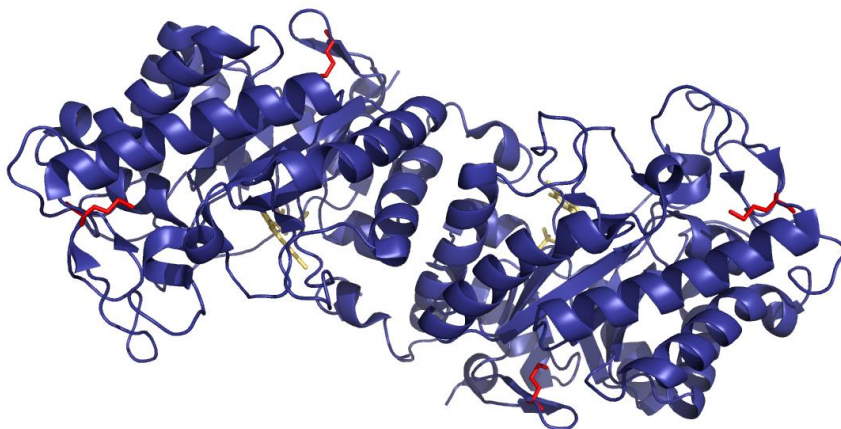


Figure 3.7. Crystal structure of YqjM (pdb: 1z48) with the oxidised amino acids marked in red.

3.4. Conclusions

Overall, we have confirmed that direct, NAD(P)H-independent regeneration of YqjM can productively be achieved using photoregenerated, reduced FMN photocatalysts/mediators.

The main limitation of the current setup lies with the poor photostability of the enzyme-bound, as well as the free FMN cofactor. Consequently, comparably low turnover numbers ($TN = \text{mol}_{\text{Product}} \times \text{mol}_{\text{Catalyst}}^{-1}$) in the range of 2000 and 30-40 for YqjM and FMN, respectively, were observed. While these numbers are in the range of state-of-the-art OYE reactions^{3, 60, 61} they are orders of magnitude too low for economical synthesis of non-highly value-added products.⁶² Therefore, further work will have to concentrate on increasing the robustness of the photoenzymatic reaction. Particularly we will focus on photocatalysts/mediators such as methylene blue and its derivatives,⁶³ exhibiting an absorption maximum in the (infra)red range. This way, the photodegradation of OYEs can be minimised. Ideally, these photocatalysts/mediators exhibit more efficient interaction with the enzyme active

site to accelerate the electron transfer from the reduced mediator to the oxidised enzyme-bound flavin.⁶⁴

3.5. References

1. O. Warburg, W. Christian, *Biochem. Z.*, 1933, **263**, 228-229.
2. R. Stürmer, B. Hauer, M. Hall, K. Faber, *Curr. Opin. Chem. Biol.*, 2007, **11**, 203-2013.
3. M. Hall, C. Stueckler, W. Kroutil, P. Macheroux, K. Faber, *Angew. Chem. Int. Ed.*, 2007, **46**, 3934-3937.
4. H.S. Toogood, J.M. Gardiner, N.S. Scrutton, *ChemCatChem*, 2010, **2**, 892-914.
5. H.S. Toogood, N.S. Scrutton, *Curr. Opin. Chem. Biol.*, 2014, **19**, 107-115.
6. U. Karl, A. Simon, *Chimica Oggi*, 2009, **27**.
7. H.S. Toogood, N.S. Scrutton, *ACS Catal.*, 2018, **8**, 3532-3549.
8. H.S. Toogood, T. Knaus, N.S. Scrutton, *ChemCatChem*, 2013, **6**, 951-954.
9. T. Knaus, C.E. Paul, C.W. Levy, S. de Vries, F.G. Mutti, F. Hollmann, N.S. Scrutton, *J. Am. Chem. Soc.*, 2016, **138**, 1033-1039.
10. A. Geddes, C.E. Paul, S. Hay, F. Hollmann, N.S. Scrutton, *J. Am. Chem. Soc.*, 2016, **138**, 11089-11092.
11. C.E. Paul, S. Gargiulo, D.J. Opperman, I. Lavandera, V. Gotor-Fernandez, V. Gotor, A. Taglieber, I.W.C.E. Arends, F. Hollmann, *Org. Lett.*, 2013, **15**, 180-183.
12. I. Zachos, C. Nowak, V. Sieber, *Curr. Opin. Chem. Biol.*, 2019, **49**, 59-66.
13. J. Bernard, E. van Heerden, I.W.C.E. Arends, D.J. Opperman, F. Hollmann, *ChemCatChem*, 2012, **4**, 196-199.
14. Y. Okamoto, V. Köhler, C.E. Paul, F. Hollmann, T.R. Ward, *ACS Catal.*, 2016, **6**, 3553-3557.
15. M.K. Peers, H.S. Toogood, D.J. Heyes, D. Mansell, B.J. Coe, N.S. Scrutton, *Catal. Sci. Technol.*, 2015, **6**, 169-177.
16. T.N. Burai, A.J. Panay, H. Zhu, T. Lian, S. Lutz, *ACS Catal.*, 2012, **2**, 667-670.
17. M. Mifsud Grau, J.C. van der Toorn, L.G. Otten, P. Macheroux, A. Taglieber, F.E. Zilly, I.W.C.E. Arends, F. Hollmann, *Adv. Synth. Catal.*, 2009, **351**, 3279-3286.
18. M. Mifsud, S. Gargiulo, S. Iborra, I.W.C.E. Arends, F. Hollmann, A. Corma, *Nat. Commun.*, 2014, **5**.
19. A. Bachmeier, B.J. Murphy, F.A. Armstrong, *J. Am. Chem. Soc.*, 2014, **136**, 12876-12879.
20. J. Yoon, S.H. Lee, F. Tieves, M.C.R. Rauch, F. Hollmann, C.B. Park, *ACS Sustain. Chem. Eng.*, 2019, **7**, 5632-5637.
21. M.M.C.H. van Schie, S. Younes, M.C.R. Rauch, M. Pesic, C.E. Paul, I.W.C.E. Arends, F. Hollmann, *Molecular Catalysis*, 2018, **452**, 277-283.
22. E.J. Son, S.H. Lee, S.K. Kuk, M. Pesic, D.S. Choi, J.W. Ko, K. Kim, F. Hollmann, C.B. Park, *Adv. Funct. Mater.*, 2018, **28**, 1705232.
23. J. Kim, S.H. Lee, F. Tieves, D.S. Choi, F. Hollmann, C.E. Paul, C.B. Park, *Angew. Chem. Int. Ed.*, 2018, **52**, 13825-13828.
24. J. Qi, C.E. Paul, F. Hollmann, D. Tischler, *Enz. Microb. Technol.*, 2017, **100**, 17-19.

25. S.H. Lee, D.S. Choi, M. Pesic, Y. Woo, C.E. Paul, F. Hollmann, C.B. Park, *Angew. Chem. Int. Ed.*, 2017, **56**, 8681-8685.
26. A. Taglieber, F. Schulz, F. Hollmann, M. Rusek, M.T. Reetz, *ChemBioChem*, 2008, **9**, 565-572.
27. W.R. Frisell, C.G. Mackenzie, *Proc. Natl. Acad. Sci. U. S. A.*, 1959, **45**, 1568-1572.
28. W.R. Frisell, C.W. Chung, C.G. Mackenzie, *J. Biol. Chem.*, 1959, **234**, 1297-1302.
29. V. Massey, M. Stankovitch, P. Hemmerich, *Biochem.*, 1978, **17**, 1-8.
30. V. Massey, P. Hemmerich, *Biochem.*, 1978, **17**, 9-16.
31. W.R. Knappe, P. Hemmerich, H.J. Duchstein, H. Fenner, V. Massey, *Biochem.*, 1978, **17**, 16-17.
32. M. Pesic, E. Fernández-Fueyo, F. Hollmann, *ChemistrySelect*, 2017, **2**, 3866-3871.
33. T.B. Fitzpatrick, S. Auweter, K. Kitzing, T. Clausen, N. Amrhein, P. Macheroux, *Prot. Express. Purif.*, 2004, **36**, 280-291.
34. T.B. Fitzpatrick, N. Amrhein, P. Macheroux, *J. Biol. Chem.*, 2003, **278**, 19891-19897.
35. T. Classen, M. Korpak, M. Scholzel, J. Pietruszka, *ACS Catal.*, 2014, **4**, 1321-1331.
36. F. W. Studier, *Methods Mol. Biol.*, 2014, **1091**, 17-32.
37. F.W. Studier, *Prot. Express. Purif.*, 2005, **41**, 207-234.
38. V. Massey, *J. Biol. Chem.*, 1994, **269**, 22459-22462.
39. M.M.C.H. van Schie, C.E. Paul, I.W.C.E. Arends, F. Hollmann, *Chem. Commun.*, 2019, **55**, 1790-1792.
40. G.T. Höfler, E. Fernández-Fueyo, M. Pesic, S.H. Younes, E.-G. Choi, Y.H. Kim, V.B. Urlacher, I.W.C.E. Arends, F. Hollmann, *ChemBioChem*, 2018, **19**, 2344-2347.
41. M.C.R. Rauch, S. Schmidt, I.W.C.E. Arends, K. Oppelt, S. Kara, F. Hollmann, *Green Chem.*, 2017, **19**, 376-379.
42. D. Holtmann, F. Hollmann, *ChemBioChem*, 2016, **17**, 1391-1398.
43. S. Gargiulo, I.W.C.E. Arends, F. Hollmann, *ChemCatChem*, 2011, **3**, 338-342.
44. M. Insinska-Rak, A. Golczak, M. Sikorski, *J. Phys. Chem. A*, 2012, **116**, 1199-1207.
45. A. Penzkofer, A. Tyagi, J. Kiermaier, *J. Photochem. Photobiol. A*, 2011, **217**, 369-375.
46. W. Holzer, J. Shirdel, P. Zirak, A. Penzkofer, P. Hegemann, R. Deutzmann, E. Hochmuth, *Chem. Phys.*, 2005, **308**, 69-78.
47. S. Pill-Soon, D.E. Metzler, *Photochem. Photobiol.*, 1967, **6**, 691-709.
48. W. Stampfer, B. Kosjek, K. Faber, W. Kroutil, *J. Org. Chem.*, 2003, **68**, 402-406.
49. B. Kosjek, W. Stampfer, R.V. Deursen, K. Faber, W. Kroutil, *Tetrahedron*, 2003, **59**, 9517-9521.
50. V.I. Tishkov, V.O. Popov, *Biomol. Eng.*, 2006, **23**, 89-110.
51. V.I. Tishkov, V.O. Popov, *Biochemistry. Mosc.*, 2004, **69**, 1252-1267.
52. E. Schmidt, O. Ghisalpa, D. Gyax, G. Sedelmeier, *J. Biotechnol.*, 1992, **24**, 315-327.
53. J. Sucharitakul, C. Tongsook, D. Pakotiprapha, W.J.H. van Berkel, P. Chaiyen, *J. Biol. Chem.*, 2013, **288**, 35210-35221.
54. S. Montersino, R. Orru, A. Barendregt, A.H. Westphal, E. van Duijn, A. Mattevi, W.J.H. van Berkel, *J. Biol. Chem.*, 2013, **288**, 26235-26245.
55. S. Montersino, W.J.H. van Berkel, *Biochim. Biophys. Acta, Proteins Proteomics*, 2012, **1824**, 433-442.

56. A.A. Arifin, M.M. Don, M.H. Uzir, *Biochem. Eng. J.*, 2011, **56**, 219-224.
57. E.M. Buque-Taboada, A.J.J. Straathof, J.J. Heijnen, L.A.M. van der Wielen, *Adv. Synth. Catal.*, 2005, **347**, 1147-1154.
58. T.C. Squier, *Exp. Gerontol.*, 2001, **36**, 1539-1550.
59. A. Scholtissek, E. Gädke, C.E. Paul, A.H. Westphal, W.J.H. van Berkel, D. Tischler, *Front. Microbiol.*, 2018, **9**.
60. C.K. Winkler, K. Faber, M. Hall, *Curr. Opin. Chem. Biol.*, 2018, **43**, 97-105.
61. C. Stueckler, T.C. Reiter, N. Baudendistel, K. Faber, *Tetrahedron*, 2010, **66**, 663-667.
62. P. Tufvesson, J. Lima-Ramos, M. Nordblad, J.M. Woodley, *Org. Proc. Res. Dev.*, 2010, **15**, 266-274.
63. S.J.P. Willot, E. Fernández-Fueyo, F. Tieves, M. Pesic, M. Alcalde, I.W.C.E. Arends, C.B. Park, *ACS Catal.*, 2019, **9**, 890-894.
64. F.W. Strohle, S.Z. Cekic, A.O. Magnusson, U. Schwaneberg, D. Roccatano, J. Schrader, D. Holtmann, *J. Mol. Catal. B Enzym.*, 2013, **88**, 47-51.

Chapter 4:

Metals in biotechnology: Cr-driven-stereoselective reduction of conjugated C=C-double bonds

Elementary metals are shown to be suitable sacrificial electron donors to drive stereoselective reduction of conjugated C=C-double bonds using old yellow enzymes as catalysts. Both, direct electron transfer from the metal to the enzyme as well as mediated electron transfer is feasible, though the latter excels by higher reaction rates. The general applicability of this new chemoenzymatic reduction method is demonstrated as well as current limitations are outlined.

This chapter is based on

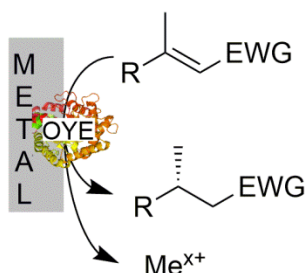
M.C.R. Rauch, Y. Gallou, L. Delorme, C.E. Paul, I.W.C.E. Arends, F. Hollmann, *ChemBioChem*, 2019, **20**, 1-5.

4.2. Introduction

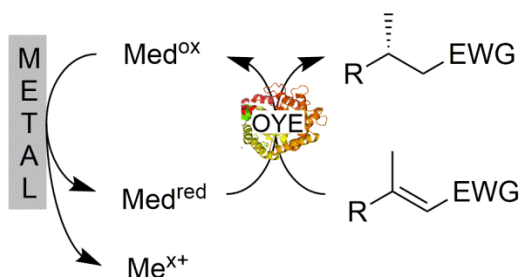
In recent years, so-called *Old Yellow Enzymes* (OYEs) have attracted significant attention as catalysts for the stereoselective reduction of conjugated C=C-double bonds.¹ To maintain their catalytic cycle, OYEs depend on a continuous supply with reducing equivalents, which classically originate from the natural nicotinamide adenine dinucleotide cofactors NAD(P)H. In addition to these, a range of alternative regeneration approaches have been developed^{1j, 2} Such alternate hydride sources range from synthetic nicotinamide mimics³ to electrochemical supplies.⁴

Elementary metals represent another, potentially useful source of reducing equivalents to drive OYE-catalysed reduction reactions. To the best of our knowledge, apart from some pioneering works by Schwaneberg et al.,⁵ this approach has not been explored further in redox biocatalysis.

a) direct reduction pathway



b) indirect reduction pathway



Scheme 4.1. Metal-driven regeneration of OYE via either a) direct electron transfer to the enzyme-bound prosthetic group or b) indirectly using a low-molecular-weight mediator.

We therefore decided to explore the potential of elementary metals to promote OYE-catalysed reduction reactions (Scheme 4.1). Principally, two mechanisms can be imagined for the electron transfer from the metal to the enzyme-bound flavin prosthetic group. Either direct electron transfer occurs or, since the prosthetic group is usually buried deeply within the protein, indirect electron transfer via a low-molecular weight mediator is established.

4.2. Material and methods

4.2.1. Chemicals

Unless stated otherwise all chemicals were purchased from Sigma-Aldrich and TCI and were used without further purification. Columns and column material for enzyme purification were purchased from GE Healthcare.

4.2.2. Enzyme preparation.

Recombinant expression and purification of YqjM from *Bacillus subtilis* was performed following a previously described procedure.^{6c}

4.2.3. Chemoenzymatic reactions.

Each reaction was carried out under strict anaerobic conditions (glovebox) in 1.5 mL glass vials with a working volume of 400 μ L. Stirring bars were used for suspending the metals in the reaction. Reactions with mediators were protected from light with aluminium foil.

4.2.4. XPS analysis.

The used XPS was a Thermofisher K-Alpha. The X-ray gun uses an Al K α source with an energy of 1486 eV. The (nominal) spot size was set to 400 μ m. During the measurements a flood gun was used for charge compensation, setting the pressure to approx. $5 \cdot 10^{-7}$ mbar.

4.3. Results and discussion

As a model enzyme we chose the OYE homologue from *Bacillus subtilis* (YqjM).⁶ For this, we evaluated pathway **a**, *i.e.* direct electron transfer by incubating purified YqjM in the presence of a metal and recording UV spectra of the reaction mixture overtime. Particularly, elementary zinc and chromium gave positive results (Figure 4.1). The disappearance of the characteristic peak around 450 nm for the oxidised flavin prosthetic group served as analytical signal to detect electron transfer.

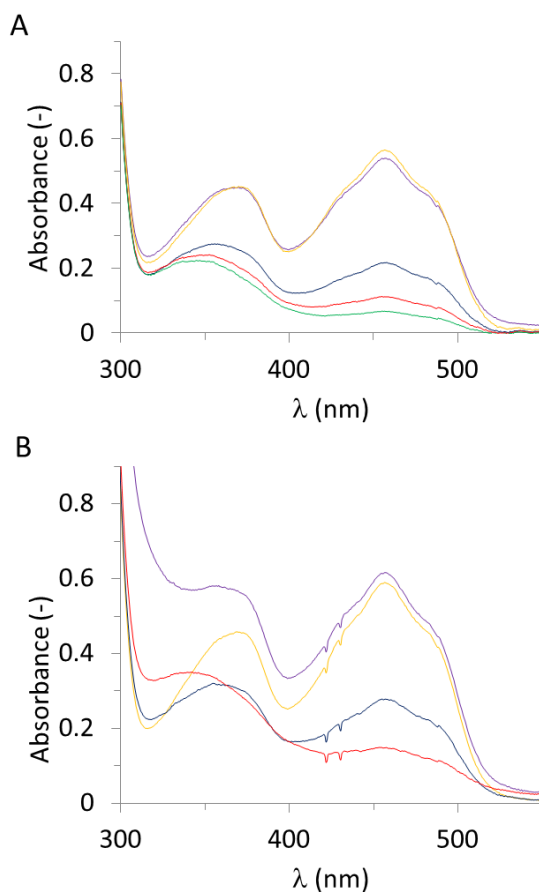


Figure 4.1. Direct reduction of YqjM using Zn (A) or Cr (B) as reductant. Conditions: [purified YqjM] = 50 μ M in KPi buffer 100 mM pH 6.5, 65 mg/mL of zinc powder <10 μ m or 50 mg/mL of chromium powder <45 μ m, 21 $^{\circ}$ C. Spectra were recorded at intervals (A): 0 min (yellow), 10 min (blue), 20 min (red), 30 min (green) and after reoxidation (purple); B: 0 h (yellow), 6 h (blue), 23 h (red) and after reoxidation (purple, note that the FMN spectrum is overlaid by the presence of Cr^{2+}).

Interestingly, whereas YqjM was fully reduced within minutes in the presence of Zn, (Figure 4.1A), it took several hours to fully reduce YqjM with Cr (Figure 4.1B). The exact reason for this is unclear but the lower particle size of the Zn metal used here may account for this. Interestingly, the standard redox potential does not seem to have a decisive influence ($E^\circ (\text{Zn}/\text{Zn}^{2+}) = -0.76 \text{ V}_{\text{NHE}}$, $E^\circ (\text{Cr}/\text{Cr}^{2+}) = -0.9 \text{ V}_{\text{NHE}}$). It is worth mentioning that upon aeration the spectrum of the oxidised flavin prosthetic group was fully restored indicating that the reduction by the metals had no detrimental effect on the enzyme integrity.

However, performing chemoenzymatic reductions of 2-methylcyclohexenone with Zn as sacrificial electron donor yielded only very poor optical purities of the products. We attributed this to a significant non-enzymatic background reduction yielding racemic products, which we also confirmed in the corresponding control reactions. Therefore, for all further reactions, we used Cr as sacrificial electron donor. Similar to YqjM, further OYEs such as the ScOYE2 from *Saccharomyces cerevisiae* and TsOYE from *Thermus scotoductus* were also reduced directly by Cr and catalytically reduced 2-methylcyclohexenone (Table 4.1).

Table 4.1. Enzyme scope of the regeneration of OYEs by chromium. Conditions: [purified enzyme] = 6.9 μM in KPi buffer 100 mM pH 6.5, [2-methylcyclohex-2-en-1-one] = 10 mM, 50 mg/mL of chromium powder <45 μm , 21 $^\circ\text{C}$. Data presented are an average of duplicates.

Enzyme	Product formation (mM)	TF (h^{-1})
YqjM	0.40	0.80
ScOYE2	0.51	1.45
TsOYE	0.16	0.45

In view of the rather sluggish reduction kinetics using Cr metal alone (Figure 4.1), we investigated several mediators (Scheme 4.1B). As shown in Figure 4.2, all redox active mediators tried significantly improved the product formation approximately 10-fold compared with the direct, non-mediated reduction.

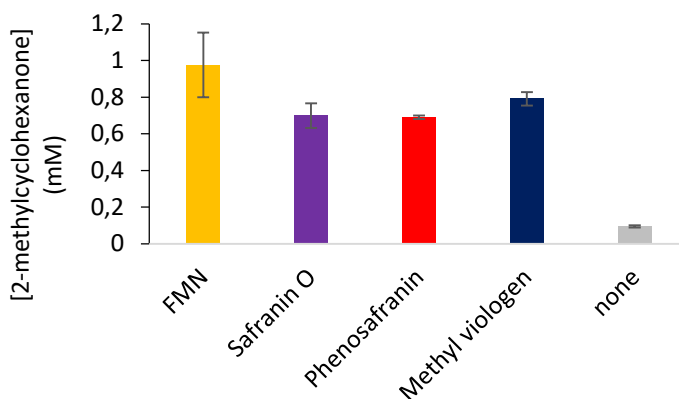


Figure 4.2. Chemoenzymatic reduction of 2-methylcyclohexanone in the presence/absence of low-molecular weight redox mediators. Conditions: [purified YqjM] = 6.9 μ M, [2-methylcyclohex-2-en-1-one] = 10 mM, 50 mg/mL of chromium powder <45 μ m, [mediator] = 500 μ M in KPi buffer 100 mM pH 6.5, 21 $^{\circ}$ C, reaction time of 4 hours. Data presented are an average of duplicates.

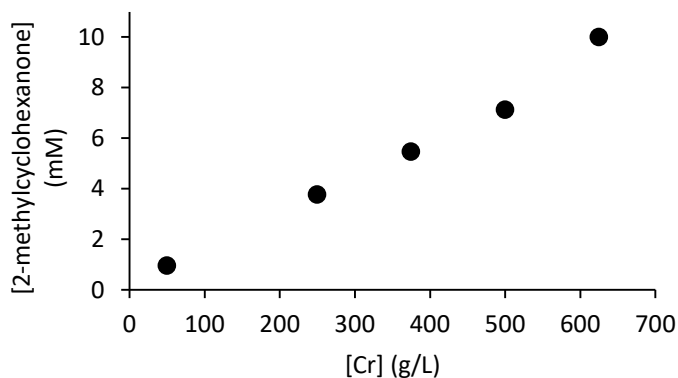


Figure 4.3. Influence of the Cr amount used on the overall product formation. Conditions: [purified YqjM] = 6.9 μ M, [FMN] = 500 μ M in KPi buffer 100 mM pH 6.5, [2-methylcyclohex-2-en-1-one] = 10 mM, chromium powder <45 μ m, 21 $^{\circ}$ C. Data presented are averages of duplicates.

We therefore performed all further experiments using FMN as mediator. In a next step, we investigated the influence of the amount of the reductant (Cr) on the overall performance of the reduction reaction. As shown in Figure 4.3, an almost linear relationship between amount of Cr and the final product concentration was observed. It must, however, be noted that a 1000-fold molar excess of Cr over the

starting material was necessary to attain full conversion. A plausible explanation for this observation may be that passivation of the metal surface prevented the bulk metal from being used for the reduction of FMN. Additionally, the Cr metal used in this study was already partially passivated as XPS analysis revealed a Cr⁰-surface content of approximately 5.5% (after a reaction this value was reduced to 1.2%).

Table 4.2. Substrate scope of the chemoenzymatic reduction.

Product	Concentration (mM)	Conversion (%)	Yield (%)	ee (%)
	8.6	81	81	65 (R)
	6.9	70	70	85 (S)
	7.3	70	70	>99 (R)
	6.7	77	77	-
	2.8	26	26	n.d
	0.6	85	6	>99 (2R,5S)

Conditions: [purified YqjM] = 6.9 μ M, [FMN] = 500 μ M in KPi buffer 100 mM pH 6.5, [substrate] = 10 mM, 500 mg/mL of chromium powder <45 μ m, 21 $^{\circ}$ C, reaction time of 4 hours. n.d. = not determined; conversion = $([\text{starting material}]_0 - [\text{starting material}]_{4\text{h}}) \times [\text{starting material}]_0^{-1}$; yield = $[\text{product}]_{4\text{h}} \times \Sigma[\text{all reagents}]_{4\text{h}}^{-1}$.

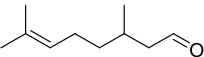
The product scope of the proposed chemoenzymatic reaction was very comparable to the scope determined previously.^{6c, 7} Also the enantioselectivities were comparable with the exception of levodione and citronellal where the enantiomeric excess (ee)-values of the chemoenzymatic reaction system were significantly lower than those obtained using NAD(P)H as reductant. Control experiments in the

absence of YqjM revealed a significant background activity (formation of racemic reduction product) which can be attributed to the direct, non-enzymatic reduction by the reduced mediator (Table 4.2). Similar observations have been reported by Scrutton and coworkers.⁸ Interestingly, no such side reaction was observed using Cr alone as reductant.

The evaluation of the substrate scope (Table 4.2) also revealed the generally very high chemoselectivity of the proposed reaction scheme. For the reduction of carvone, control experiments showed that the poor chemoselectivity here can be attributed to the direct, non-enzymatic reduction of the non-conjugated C=C-double bond by the reduced mediator. Once more, no such side reaction was observed using Cr alone as reductant.

Traditional, *i.e.* NAD(P)H-dependent, regeneration systems are challenged by poor selectivity as well. Especially when using crude (*i.e.* non-purified) enzyme preparations, over-reduction of the carbonyl group is frequently observed, in particular with conjugated aldehydes as starting materials.⁹ As the reaction system proposed here does not regenerate reduced nicotinamide cofactors, this undesired side reaction should play no role here. We therefore also tested crude cell extracts of recombinant *E. coli* cells overexpressing YqjM as biocatalyst preparation for the reduction of 2-methylcyclohex-2-en-1-one and citral. In both cases, the saturated ketone and aldehydes were observed as sole products without formation of the undesired alcohol by-products (Table 4.3).

Table 4.3. Characterisation of the use of CFE YqjM. [CFE YqjM] = 6.9 μ M, [FMN] = 500 μ M in KPi buffer 100 mM pH 6.5, [substrate] = 10 mM, 500 mg/mL of chromium powder <45 μ m, 21 $^{\circ}$ C, reaction time of 4 hours. Data presented are an average of duplicates.

Expected product	Product concentration (mM)	Yield (%)	<i>ee</i> (%)
2-methylcyclohexanone 	4.4	42	93 (<i>R</i>)
Citronellal 	1.5	16	n.d.

Yield = [expected product] / [substrate]₀

n.d. = not determined.

4.4. Conclusions

Overall, in this contribution we have demonstrated that elementary metals can serve as sacrificial reductants to promote OYE-catalysed C=C-bond reductions. Though the direct, non-mediated electron transfer to the enzymes was feasible, it was greatly accelerated by the application of redox mediators. The high chemoselectivity of nicotinamide-independent regeneration systems was preserved. This approach may particularly prove useful for substrate screening campaigns.

The current system, apparently, needs further improvements in order to become truly practical. First and foremost, using Cr as stoichiometric reductant does not appear to be a truly green method, especially considering the need for high molar surpluses and the release of questionable metal ions into the reaction medium. We envision that mixed valence state oxides or sulphides may be more practical alternatives to elementary metals as here the release of metal ions into the reaction medium may be avoided. Also, the particles can principally be recharged electrochemically and re-used.

4.5. References

- 1 a) O. Warburg, W. Christian, *Biochem. Z.*, 1933, **263**, 228-229; b) B.A. Palfey, V. Massey, in *Radical Reactions and Oxidation / Reduction, Vol. III* (Ed.: M. Sinnott), Academic Press, San Diego, London, 1998, 83-154; c) W.J.H. Van Berkel, in *Wiley Encyclopedia of Chemical Biology*, 2018; d) V. Joosten, W.J.H. van Berkel, *Curr. Opin. Chem. Biol.*, 2007, **11**, 195-202; e) B.M. Nestl, S.C. Hammer, B.A. Nebel, B. Hauer, *Angew. Chem. Int. Ed.*, 2014, **53**, 3070–3095; f) B.M. Nestl, B.A. Nebel, B. Hauer, *Curr. Opin. Chem. Biol.*, 2011, **15**, 187-193; g) R. Stürmer, B. Hauer, M. Hall, K. Faber, *Curr. Opin. Chem. Biol.*, 2007, **11**, 203-213; h) H.S. Toogood, N.S. Scrutton, *ACS Catal.*, 2018, **8**, 3532-3549; i) H.S. Toogood, N.S. Scrutton, *Curr. Opin. Chem. Biol.*, 2014, **19**, 107-115; j) H.S. Toogood, T. Knaus, N.S. Scrutton, *ChemCatChem*, 2013, **6**, 951–954; k) H.S. Toogood, J.M. Gardiner, N.S. Scrutton, *ChemCatChem*, 2010, **2**, 892–914.
- 2 W. Zhang, F. Hollmann, *Chem. Commun.*, 2018, **54**, 7281-7289.
- 3 a) J. Kim, S.H. Lee, F. Tieves, D.S. Choi, F. Hollmann, C.E. Paul, C.B. Park, *Angew. Chem. Int. Ed.*, 2018, **130**, 14021-14024; b) C.E. Paul, F. Hollmann, *Appl. Microbiol. Biotechnol.*, 2016, **100**, 4773–4778; c) T. Knaus, C.E. Paul, C.W. Levy, S. de Vries, F.G. Mutti, F. Hollmann, N.S. Scrutton, *J. Am. Chem. Soc.*, 2016, **138**, 1033–1039; d) C.E. Paul, I.W.C.E. Arends, F. Hollmann, *ACS Catal.*, 2014, **4**, 788–797; e) C.E. Paul, S. Gargiulo, D.J. Opperman, I. Lavandera, V. Gotor-Fernandez, V. Gotor, A. Taglieber,

- I.W.C.E. Arends, F. Hollmann, *Org. Lett.*, 2013, **15**, 180-183; f) J. Qi, C.E. Paul, F. Hollmann, D. Tischler, *Enz. Microb. Technol.*, 2017, **100**, 17-19.
- 4 a) D. Holtmann, S. Bormann, M.M.C.H. van Schie, T.P. De Almeida, W. Zhang, M. Stöckl, R. Ulber, F. Hollmann, *ChemSusChem* 2019, DOI: 10.1002/cssc.201902326; b) A.E.W. Horst, S. Bormann, J. Meyer, M. Steinhagen, R. Ludwig, A. Drews, M. Ansorge-Schumacher, D. Holtmann, *J. Mol. Catal. B: Enzym.*, 2016, **133**, S137-S142; c) S. Lutz, E. Steckhan, A. Liese, *Electrochem. Commun.*, 2004, **6**, 583-587.
- 5 U. Schwaneberg, D. Appel, J. Schmitt, R.D. Schmid, *J. Biotechnol.*, 2000, **84**, 249-257.
- 6 a) K. Kitzing, T.B. Fitzpatrick, C. Wilken, J. Sawa, G.P. Bourenkov, P. Macheroux, T. Clausen, *J. Biol. Chem.*, 2005, **280**, 27904-27913; b) T.B. Fitzpatrick, N. Amrhein, P. Macheroux, *J. Biol. Chem.*, 2003, **278**, 19891-19897; c) M. Pesic, E. Fernández-Fueyo, F. Hollmann, *ChemistrySelect*, 2017, **2**, 3866-3871.
- 7 M. Hall, C. Stückler, H. Ehammer, E. Pointner, G. Oberdorfer, K. Gruber, B. Hauer, R. Stürmer, W. Kroutil, P. Macheroux, K. Faber, *Adv. Synth. Catal.*, 2008, **350**, 411-418.
- 8 M.K. Peers, H.S. Toogood, D.J. Heyes, D. Mansell, B.J. Coe, N.S. Scrutton, *Catal. Sci. Technol.*, 2015, **6**, 169-177.
- 9 M. Hall, B. Hauer, R. Stuermer, W. Kroutil, K. Faber, *Tetrahedron Asymm.*, 2006, **17**, 3058-3062.

Chapter 5:

Peroxygenase-catalysed epoxidation of styrene derivatives in neat reaction media

Biocatalytic oxyfunctionalisation reactions are traditionally conducted in aqueous media, limiting their production yield. Here we report the application of a peroxygenase in neat reaction conditions reaching product concentrations of up to 360 mM.

This chapter is based on

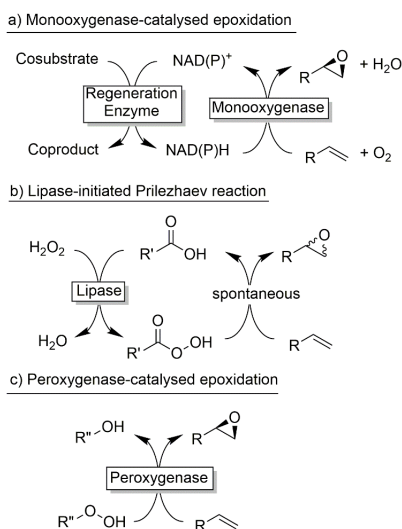
M.C.R. Rauch, F. Tieves, C.E. Paul, I.W.C.E. Arends, M. Alcalde, F. Hollmann,
ChemCatChem, 2019, **11**, 4519-4523.

5.1. Introduction

Epoxides are important building blocks in organic synthesis. The ring opening of epoxides leads to useful α - or β -substituted alcohols.¹ As a result, a broad range of catalytic methods for the epoxidation of C=C-double bonds have been established.² Compared to this variety, only few biocatalytic methods are known. The chemoenzymatic epoxidation of alkenes using lipase-borne peracids for example is receiving tremendous interest but yields racemic products.³ Amongst the stereospecific epoxidation methods the use of flavin-dependent styrene monooxygenases⁴ and P450 monooxygenases⁵ are most prominent.

The latter approaches rely on reductive activation of molecular oxygen using reduced nicotinamide cofactors (NAD(P)H) as source of reducing equivalents. This not only implies complicated and vulnerable electron transport chains but also, due to the exclusive water-solubility of the cofactors, largely limits these processes to aqueous reaction media.

The majority of the alkenes of interest are however hydrophobic, limiting the final product titres to the lower millimolar range. This is unacceptable from an economic and an environmental point-of-view. Current solutions focus around two-liquid-phase-system approaches (2LPS)⁶



Scheme 5.1. Comparison of biocatalytic epoxidation reactions.

Ideally, (bio)catalytic epoxidation reactions should occur in organic media (even neat) to enable high product concentrations. In this respect, peroxygenases represent a promising solution.⁷ Peroxygenases are heme-thiolate enzymes enabling P450 monooxygenase-like oxyfunctionalisation reactions. In contrast to monooxygenases, peroxygenases do not rely on (water-soluble) redox partners but on (organic) peroxides, enabling their potential application in non-aqueous media. Pioneering works by Pu, Wang and Zhang⁸ and Hofrichter⁹ have established peroxygenase-catalysed epoxidation reactions using hydrogen peroxide or organic hydroperoxides as oxidants, albeit in aqueous reaction media thereby limiting the reagent concentration to the lower millimolar range.

Klibanov and coworkers reported peroxidase-reactions under non-aqueous conditions.¹⁰ Unfortunately, these contributions have not yet found widespread attention in biocatalysis. We therefore set out to establish peroxygenase-catalysed, selective oxyfunctionalisation reactions in neat reaction media.

5.2. Material and methods

5.2.1. Chemicals

Unless stated otherwise all chemicals were purchased from Sigma-Aldrich and TCI and were used without further purification. Columns and column material for enzyme purification were purchased from GE Healthcare.

5.2.2. Analytics

¹H-NMR spectroscopy:

All measurements were recorded on an Agilent 400 (400 MHz) in CDCl₃.

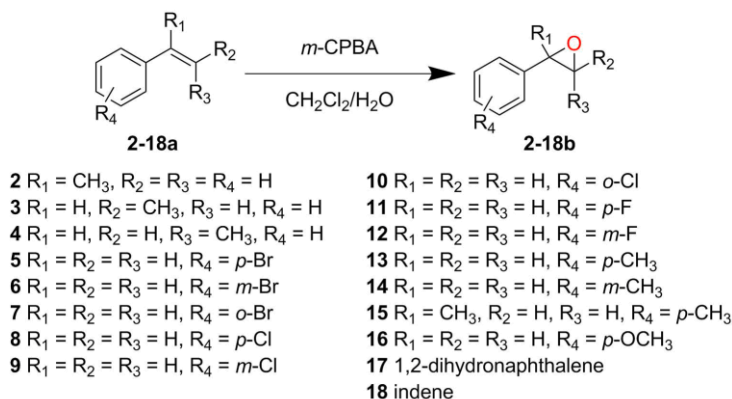
Gas chromatography (GC) analysis:

GC measurements were performed on a Shimadzu GC-14A equipped with either:

5.2.3. Enzymes

The PaDal variant of the unspecific peroxygenase (rAaeUPO) from *Agrocybe aegerita* was expressed in *Pichia pastoris* as described previously.⁹

5.2.4. Synthesis of racemic styrene oxide derivatives



Scheme 5.2. Synthesis of racemic styrene epoxide derivatives

The synthesis of several racemic epoxides was carried out according to the following procedure²: the styrene derivative (2 mmol) was diluted in CH₂Cl₂ (10 mL) and mixed with distilled water (10 mL) containing NaHCO₃ (1 g). Then, *m*-CPBA (2.2 mmol) was carefully added. The reaction mixture was stirred at room temperature for 3 hours. To quench the reaction, aqueous Na₂SO₃ (1.3 g in 10 mL) was added and left to stir for 20 min. The aqueous phase was then extracted with CH₂Cl₂ (2 x 10 mL). The combined organic phases were washed with NaHCO₃ (2 x 25 mL) and distilled water (25 mL). The organic phase was dried over anhydrous MgSO₄, filtered and evaporated under reduced pressure to afford the product. The compounds produced with this methods are: α-methylstyrene oxide **2b**, *trans*-β-methylstyrene oxide **3b**, *cis*-β-methylstyrene oxide **4b**, 4-bromostyrene oxide **5b**, 3-bromostyrene oxide **6b**, 2-bromostyrene oxide **7b**, 4-chlorostyrene oxide **8b**, 3-chlorostyrene oxide **9b**, 2-chlorostyrene oxide **10b**, 4-fluorostyrene oxide **11b**, 3-fluorostyrene oxide **12b**, 4-methylstyrene oxide **13b**, 3-methylstyrene oxide **14b**, *p*,α-dimethylstyrene oxide **15b**, 4-methoxystyrene oxide **16b**, 1,2,3,4-Tetrahydronaphthalene-1,2-oxide **17b**, indene oxide **18b**. GC and GC-MS analyses were in agreement with those published in the literature.¹¹

5.2.5. Immobilisation of rAaeUPO (PaDal) on Immobeads (IB-COV-1) from ChiralVision

10 g Immobeads (IB-COV-1) from ChiralVision were washed 3 times with 30 mL 100 mM potassium phosphate buffer pH 7.0. After mixing thoroughly with a spoon, wash was carried out at 22 °C for 5 min using overhead rotation (C2 10 rpm). The buffer was completely removed and 27.5 mL crude (44.1 µM) rAaeUPO (PaDal) was added to IB-COV-1 (50 mL falcon tube). After mixing thoroughly with a spoon, immobilisation was carried out at 22°C for 5 h using overhead rotation (C2 10 rpm). After 5 h, the immobilisation mixture was stored at 6 °C for 12 h without stirring or shaking.

After overnight incubation, the supernatant was removed and the beads 3 times washed with 10 mL 100 mM potassium phosphate buffer pH 7. The washing fractions were pooled. Samples were stored at 4 °C.

The peroxygenase concentration was determined *via* CO difference spectra in the supernatant and the washing fraction to calculate the amount of immobilised peroxygenase.

The CO difference spectrum was performed at 25 °C using 100 mM potassium phosphate buffer pH 7.0 and 50 mM sodium dithionite. Samples were bubbled with CO for 60 sec (1-2 bubbles per sec). The CO difference spectrum was recorded between 400 nm and 500 nm. From the absorbance difference between 445 nm and 490 nm, the peroxygenase concentration was calculated using an extinction coefficient of $\epsilon_{445-490} = 107 \text{ mM}^{-1} \text{ cm}^{-1}$ (AaeUPO-PaDal).

PaDal was successfully immobilised on Immobeads (IB-COV-1) from ChiralVision. Under the chosen conditions, 72.8% of the applied PaDal AaeUPO was immobilised on IB-COV-1. This corresponds to an enzyme load of 56.2 nmol/g (2.867 mg/g). The covalent immobilisation of enzymes on COV-1 enables their use in neat conditions *via* epoxide and butyl functional groups.

To estimate the catalytic activity of the immobilised rAaeUPO, an activity assay was performed using a two-liquid-phase approach: 75 µL of ethyl benzene were added to a 300 µL of a buffered solution (20 mM Tris/HCl buffer, pH 7) containing 0.5 µM of rAaeUPO (either as dissolved enzyme or immobilised). Each 30 min, 2.6

mM of t BuOOH were added. The reaction mixtures were mixed in an overhead rotator for 4 hours at ambient temperature and analysed by GC. While in case of the free enzyme more than 17 mM of product ($TF(rAaeUPO) > 2.4 \text{ s}^{-1}$) were measured, the immobilised enzyme produced only 0.53 mM of the product under otherwise identical conditions. Only 3% of the immobilised enzymes recovered activity.

5.2.6. Enzymatic reaction conditions



Figure 5.1. Picture of the reaction setup

The reactions were performed in GC-vials of 1.5 mL at room temperature, under ambient atmosphere. Immobilised rAaeUPO was first weighed in the vial according to the concentration of enzyme wanted, and then pure substrate was added to the vial. Before each sample was taken, the vial was weighed in order to estimate the loss of substrate by evaporation. t BuOOH (5.5 M in decane) was added in the vial *via* a tube connected to a syringe pump (0.91 $\mu\text{L}/\text{h}$). The system was closed to avoid evaporation as much as possible. An overhead rotator from neoLab was used for the reactions at a speed of 20 rpm. At different time points, the reactions were stopped by addition of ethyl acetate containing dodecane (5 mM) as internal standard. After extraction and centrifugation, the organic phase was dried with magnesium sulfate and analysed via gas chromatography. All concentrations reported, are based on calibration curves obtained from authentic and synthesised standards.

5.3. Results and discussion

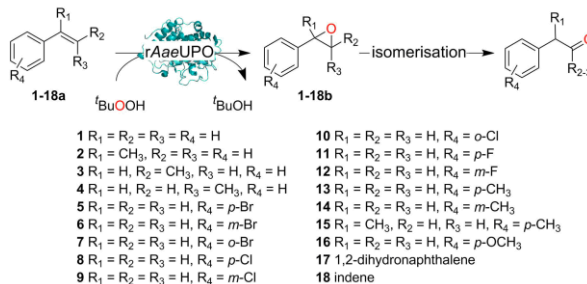
As model peroxygenase we chose an evolved recombinant peroxygenase from *Agrocybe aegerita* (rAaeUPO)¹² to catalyse the epoxidation of styrene and its derivatives.⁹ As oxidant, we chose *tert*-butyl hydroperoxide (tBuOOH) due to its high solubility in hydrophobic media.

To employ rAaeUPO in neat reaction media, we first immobilised it covalently on an epoxide-modified polyacrylic matrix (Immobead IB-COV-1). Under non-optimised conditions, 72.8% of the enzyme was immobilised. The remaining catalytic activity however was only 3%. Further development will have to focus on optimised immobilisation procedures yielding higher activity yields.

Nevertheless, having the immobilised enzyme in hand, we first explored its substrate scope (Table 5.1). Pleasingly, all of the styrene derivatives tested were converted with satisfactory to excellent turnover numbers for the biocatalyst. In accordance with previous reports^{9, 13} wild-type rAaeUPO converted the majority of styrenes non-stereoselectively giving (near racemic) epoxides, one notable exception being *cis*- β -methylstyrene, which was converted highly stereoselectively into (1*R*,2*S*)-*cis*- β -methylstyrene oxide. It is also interesting to note that in some cases, the desired epoxide was not stable and spontaneously rearranged into the corresponding carbonyl compound.

Nevertheless, very significant product concentrations of up to 100 mM were achieved. The catalytic performance of rAaeUPO in terms of turnover numbers (TON = amount of product divided by the amount of enzyme, [mol \times mol⁻¹]) was excellent.

Table 5.1. Substrate scope of the epoxidation of styrene derivatives with immobilised rAaeUPO. Data are an average of duplicates and corrected from potential substrate evaporation.



Substrate	Epoxy product (mM)	ee (%)	Carbonyl product (mM(%)) ^[a]	Time (h)	TON ^[b]	
	1a	16	12	2 (12)	42	3203
	2a	80	30	47 (37)	86	22598
	3a	9	35	1 (11)	86	1779
	4a	36	>99	2 (4)	21	6762
	5a	59	9	21 (26)	60	14235
	6a	24	50	102 (81)	62	22420
	7a	10	39	90 (90)	49	17794
	8a	8	12	22 (73)	62	5338
	9a	16	17	12 (43)	42	4982
	10a	15	15	22 (59)	22	6584
	11a	11	15	25 (69)	42	6406
	12a	3	42	1 (23)	42	712
	13a	14	- ^c	60 (81)	62	13167
	14a	36	28	59 (62)	97	16904
	15a	4	6	25 (86)	49	5160
	16a	none	-	-	-	0
	17a	136	42	147 (52)	108	50356
	18a	none	-	33 (100)	69	5872

Reaction conditions: [rAaeUPO] = 5.62 μM , $t\text{BuOOH}$ dosing rate = 5 mM/h, 20 °C, 20 rpm in overhead rotator.

[a] The concentrations of carbonyl product were calculated using the calibration curves of the epoxides. Carbonyl products are aldehyde or ketone in β position from the ring opening of the epoxides

[b] TON = [product]/[enzyme].

[c] n.d. = not determined

To identify parameters influencing the productivity of the reaction, we systematically varied the biocatalyst loading and the ^tBuOOH feeding rate in the epoxidation of *cis*- β -methylstyrene (Figure 5.2). The initial rate of the epoxidation reaction correlated directly with the dosing rate of ^tBuOOH. This however did not necessarily translate in higher product titres. Most probably, increasing feed rates of the oxidant also increased the undesired oxidative inactivation of the enzyme's active site.¹⁴ This is supported by the observation that the robustness of the reactions (i.e. the duration of product accumulation) inversely correlated with the ^tBuOOH feed rate.

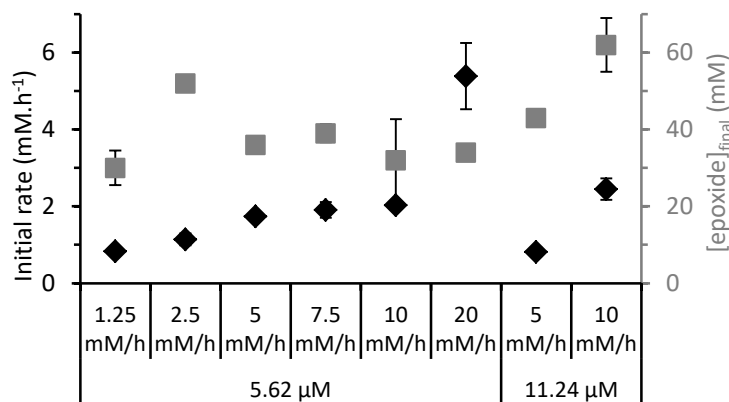
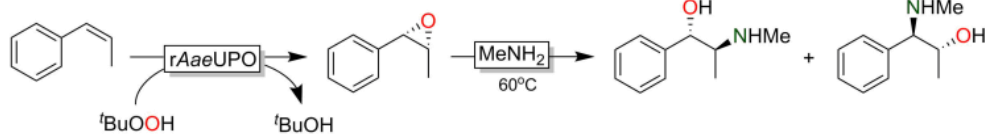


Figure 5.2. Characterisation of ^tBuOOH feeding rate and enzyme concentration comparing the initial reaction rates (black diamonds) and final product concentrations (grey squares). General conditions: room temperature, 20 rpm in overhead rotor. Data presented are an average of duplicates and corrected from potential substrate evaporation.

As mentioned above, epoxides are versatile building blocks for the synthesis of a broad range of products. Amino alcohols, for example, are common structural motifs in many pharmaceutically active ingredients.¹⁵ We therefore envisioned a chemoenzymatic cascade reaction comprising the rAaeUPO-catalysed, stereoselective epoxidation of *cis*- β -methylstyrene followed by the chemical oxirane-opening with methyl amine yielding (pseudo)ephedrine (Scheme 5.3).



Scheme 5.3. Envisioned chemoenzymatic cascade to obtain (pseudo)ephedrine from *cis*-β-methylstyrene.

The epoxidation reaction was performed on a 10 mL scale with gradual tBuOOH feed (Figure 5.3). Although a conservative tBuOOH feed rate of 5 mM h⁻¹ was applied, inactivation of the biocatalyst represented a major challenge for the reaction, necessitating further provision of the reaction with fresh enzyme (indicated by arrows in Figure 5.3). It is also interesting to note that in contrast to previous experiments using rAaeUPO in aqueous reaction media using H₂O₂,¹⁶ the peroxide utilisation efficiency was only approximately 50%. It will be interesting to further investigate this increased catalase activity of rAaeUPO.

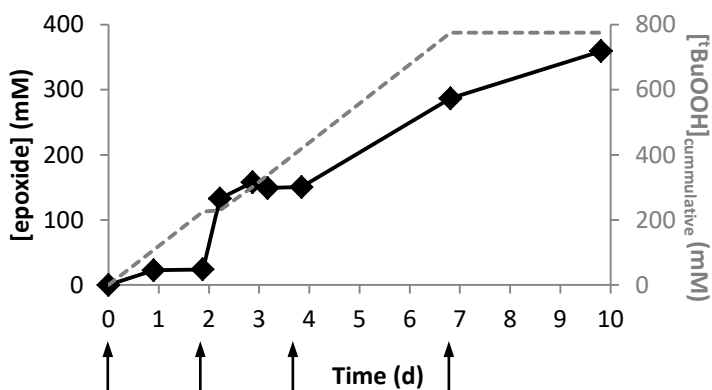
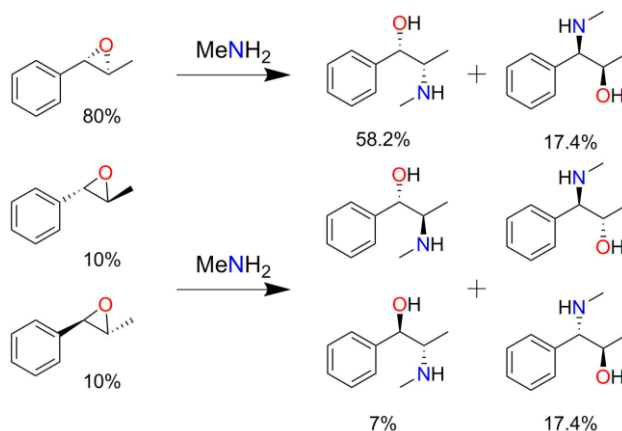


Figure 5.3. Time-course of the rAaeUPO-catalysed epoxidation of *cis*-β-methylstyrene. Conditions: 10 mL *cis*-β-methylstyrene, [rAaeUPO@IB-COV-1]_{total} = 41.8 μM (added in equal portions at the times indicated by the arrows), room temperature. tBuOOH was added continuously according to the feed profile shown as a dashed grey line.

From this experiment, 360 mM of (1R,2S)-β-methylstyrene oxide were obtained. The turnover number of the enzyme was more than 8500. Next to the desired product, the reaction mixture also contained some benzaldehyde, originating from rAaeUPO-catalysed C=C-bond cleavage.¹⁷ To avoid negative influences of this by-product, the desired product was purified chromatographically and subjected to

chemical ring-opening with methylamine resulting in pseudoephedrine (58.2%), ephedrine (7%) and isoephedrine (34.8%) (Scheme 5.4).



Scheme 5.4. Summary of the synthesis of pseudoephedrine via the ring opening of *cis*-6-methylstyrene oxide using 30 equivalents of methylamine. Percentages were determined by NMR analysis.

5.4. Conclusions

Overall, with this contribution we have demonstrated that peroxygenase-catalysed epoxidations can be performed under neat reaction conditions. This opens up new possibilities for the preparative scale-application of this promising class of enzymes. Product concentrations of up to 360 mM have been achieved representing one of the highest product titres obtained with oxidoreductase catalysis¹⁸ and certainly the highest product concentration with isolated enzymes.^{6a, 6b, 19}

Nevertheless, some issues remain to be solved *en route* to a truly preparatively useful system. First and foremost, more active immobilisates of rAaeUPO need to be found. The activity recovery of the peroxygenase needs to be improved to obtain more active catalysts.²⁰ We are confident that from the wealth of immobilisation methods available today,²¹ a suitable method will be found in our ongoing research. Also, more enantioselective rAaeUPO variants are highly desirable to broaden the scope of the reaction.

5.5. References

1. M. Pineschi, *Eur. J. Org. Chem.*, 2006, **2006**, 4979-4988.
2. a) E. M. McGarrigle, D. G. Gilheany, *Chem. Rev.*, 2005, **105**, 1563-1602; b) R. L. Davis, J. Stiller, T. Naicker, H. Jiang, K. A. Jørgensen, *Angew. Chem.*, 2014, **53**, 7406-7426, *Angew. Chem. Int. Ed.*, 2014, **53**, 7406-7426.
3. a) B. O. O. Burek, S. Bormann, F. Hollmann, J. Bloh, D. Holtmann, *Green Chem.*, 2019, **21**, 3232-3249; b) J. Dong, E. Fernández-Fueyo, F. Hollmann, C. Paul, M. Pesic, S. Schmidt, Y. Wang, S. Younes, W. Zhang, *Angew. Chem.*, 2018, **130**, 9380-9404, *Angew. Chem. Int. Ed.*, 2018, **57**, 9238-9261.
4. a) E. Romero, J. R. Gómez Castellanos, G. Gadda, M. W. Fraaije, A. Mattevi, *Chem. Rev.*, 2018, **118**, 1742-1769; b) T. Heine, W. van Berkel, G. Gassner, K.-H. van Pée, D. Tischler, *Biology*, 2018, **7**, 42; c) G. Gygli, W. J. H. van Berkel, *Curr. Biotechnol.*, 2015, **4**, 100-110; d) M. M. E. Huijbers, S. Montersino, A. H. Westphal, D. Tischler, W. J. H. van Berkel, *Arch. Biochem. Biophys.*, 2014, **544**, 2-17.
5. a) V. B. Urlacher, M. Girhard, *Trends Biotechnol.*, 2019; b) J. B. Wang, M. T. Reetz, *Nat. Chem.*, 2015, **7**, 948-949.
6. a) H. Toda, R. Imae, N. Itoh, *Adv. Synth. Catal.*, 2014, **356**, 3443-3450; b) H. Toda, R. Imae, N. Itoh, *Tetrahedron Asymm.*, 2012, **23**, 1542-1549; c) J. B. Park, B. Buehler, T. Habicher, B. Hauer, S. Panke, B. Witholt, A. Schmid, *Biotechnol. Bioeng.*, 2006, **95**, 501-512.
7. a) M. Hofrichter, R. Ullrich, *Curr. Opin. Chem. Biol.*, 2014, **19**, 116-125; b) Y. Wang, D. Lan, R. Durrani, F. Hollmann, *Curr. Opin. Chem. Biol.*, 2017, **37**, 1-9.
8. a) L. Wang, S. Wei, X. Pan, P. Liu, X. Du, C. Zhang, L. Pu, Q. Wang, *Chem. Eur. J.*, 2018, **24**, 2741-2749; b) C. Zhang, P.-X. Liu, L.-Y. Huang, S.-P. Wei, L. Wang, S.-Y. Yang, X.-Q. Yu, L. Pu, Q. Wang, *Chem. Eur. J.*, 2016, **22**, 10969-10975.
9. M. Kluge, R. Ullrich, K. Scheibner, M. Hofrichter, *Green Chem.*, 2012, **14**, 440-446.
10. a) J. S. Dordick, M. A. Marletta, A. M. Klibanov, *Proc. Natl. Acad. Sci. U. S. A.*, 1986, **83**, 6255-6257; b) A. Zaks, A. M. Klibanov, *Science*, 1984, **224**, 1249-1251.
11. C. E. Paul, D. Tischler, A. Riedel, T. Heine, N. Itoh, F. Hollmann, *ACS Catal.*, 2015, **5**, 2961-2965.
12. a) P. Molina-Espeja, S. Ma, D. M. Mate, R. Ludwig, M. Alcalde, *Enz. Microb. Technol.*, 2015, **73-74**, 29-33; b) P. Molina-Espeja, E. Garcia-Ruiz, D. Gonzalez-Perez, R. Ullrich, M. Hofrichter, M. Alcalde, *Appl. Environ. Microbiol.*, 2014, **80**, 3496-3507.
13. E. Churakova, M. Kluge, R. Ullrich, I. Arends, M. Hofrichter, F. Hollmann, *Angew. Chem. Int. Ed.*, 2011, **50**, 10716-10719.
14. B. Valderrama, M. Ayala, R. Vazquez-Duhalt, *Chem. Biol.*, 2002, **9**, 555-565.
15. G. Grogan, *Curr. Opin. Chem. Biol.*, 2018, **43**, 15-22.
16. a) F. Tieves, S. J.-P. Willot, M. M. C. H. van Schie, M. C. R. Rauch, S. H. H. Younes, W. Zhang, P. G. de Santos, J. M. Robbins, B. Bommarius, M. Alcalde, A. Bommarius, F. Hollmann, *Angew. Chem.*, 2019, **131**, 7955-7959, *Angew. Chem. Int. Ed.*, 2019, **58**, 7873-7877; b) Y. Ni, E. Fernández-Fueyo, A. G. Baraibar, R. Ullrich, M. Hofrichter, H. Yanase, M. Alcalde, W. J. H. van Berkel, F. Hollmann, *Angew. Chem.*, 2016, **128**, 809-812, *Angew. Chem. Int. Ed.*, 2016, **55**, 798-801.
17. F. G. Mutti, M. Lara, M. Kroutil, W. Kroutil, *Chem. Eur. J.*, 2010, **16**, 14142-14148.

18. a) B. Bühler, I. Bollhalder, B. Hauer, B. Witholt, A. Schmid, *Biotechnol. Bioeng.*, 2003, **82**, 833-842; b) B. Bühler, I. Bollhalder, B. Hauer, B. Witholt, A. Schmid, *Biotechnol. Bioeng.*, 2003, **81**, 683-694; c) A. Schmid, K. Hofstetter, H.-J. Feiten, F. Hollmann, B. Witholt, *Adv. Synth. Catal.*, 2001, **343**, 732-737.
19. a) K. Hofstetter, J. Lutz, I. Lang, B. Witholt, A. Schmid, *Angew. Chem. Int. Ed.*, 2004, **43**, 2163-2166; b) E. Fernández-Fueyo, Y. Ni, A. Gomez Baraibar, M. Alcalde, L. M. van Langen, F. Hollmann, *J. Mol. Catal. B. Enzym.*, 2016, **134**.
20. P. Molina-Espeja, P. Santos-Moriano, E. García-Ruiz, A. Ballesteros, F. J. Plou, M. Alcalde, *Int. J. Mol. Sci.*, 2019, **20**, 1627.
21. U. Hanefeld, L. Gardossi, E. Magner, *Chem. Soc. Rev.*, 2009, **38**, 453-468

Chapter 6:

Conclusions and recommendations

Biocatalysed redox reactions are gaining interest from synthetic organic chemists. Because of their regio-, chemo- and stereoselective properties, protective groups are not necessary and thus the number of reaction steps leading to the final products can be reduced. Moreover reactions catalysed by enzymes can be carried out under mild conditions. Now that the number of enzymes that become available is increasing, the number of applications of *in vitro* enzymes is also increasing. However, as mentioned in the introduction, enzyme-catalysed reactions also have limitations, that need to be addressed. In this thesis, we studied three biocatalytic systems within the purpose of bringing them to preparative scale. The main challenge tackled is coupled to the dependency of oxidoreductases on cofactors.

Advantages and disadvantages of the oxidoreductase systems studied in terms of upscaling

Expensive nicotinamide cofactors are commonly consumed by oxidoreductases. **Chapter 2** gives an approach for the *in situ* regeneration of NAD(P)⁺ with light. Current regeneration systems for the oxidised nicotinamide cofactors require generally another enzyme and a sacrificial substrate, such as acetone and alcohol dehydrogenase¹⁻⁴ or oxygen and NAD(P)H oxidase⁵⁻⁸. In comparison, our system requires only a mediator, such as FMN and a LED light source. It allows for a reduction of the costs compared with the usual cofactors regeneration systems. Obviously, the use of catalytic amounts of NADH makes this system attractive on preparative scale from an economical point of view. The novelty of this system is the use of the cheap LED light source. Besides being less energy intensive, the significant advantage thereof, compared to the conventional white light bulb is that no real temperature control is required due to small thermal effect.

In **Chapter 3**, we circumvented the need of cofactors by directly regenerating the flavoprotein. This system has been reported before with a white light bulb as light source⁹. By using blue LEDs, we improved and up scaled the photoregeneration of OYEs using flavins and a sacrificial electron donor. As in Chapter 2, the application of LEDs leads to lower the costs because of the absence of a thermal effect. This oxidoreductase system, completely independent of NADPH is highly valued for its

preparative potential. To the best of our knowledge, from the cofactor-independent systems reported in literature, ours has the higher product concentration (36 mM). The reaction is time limited due to the degradation of the enzymes, we therefore further characterised the photoregeneration of flavoproteins and determined that the well-known photodegradation of FMN is also occurring in flavoproteins.

To circumvent the photodegradation of enzymes with light, **Chapter 4** reports a novel regeneration system for Old Yellow Enzyme using metals as reductants. Metals are used since decades in organic chemistry as reductant in redox reactions. In our system, we used zinc and chromium for the activation of flavins and flavoproteins. The activity of OYE is not declining overtime in presence of these metals. Nevertheless, some issues still need to be dealt with. High amount of metals are required in order to reach high conversions. Moreover metals like zinc display a high background activity for the reduction of substrates. Advantageously, as for the photoregeneration of Old Yellow Enzymes, cell-free extract (CFE) can be used instead of purified enzymes. No disturbance by side reactions from the ketoreductases present in the cells was observed. This is because ketoreductases are not regenerated in this system. The fact that cell-free extract can be employed is an economical advantage as purification steps are expensive.

Working in neat organic solvent, using exclusively the substrate as medium, would be ideal for applied enzymatic processes. But as cofactors are mainly water soluble, water is used as reaction medium. Only a few biocatalytic reactions have been reported to be active under these conditions¹⁰⁻¹¹. Peroxygenases accept organic cofactors, such as *tert*-butyl hydroperoxide that are soluble in organic solvents. Consequently, we applied the peroxygenases in **Chapter 5** under neat reaction conditions. With immobilised enzymes, high product concentrations (up to 360 mM) and high turnover numbers are reached in this way. In our case, (chiral) epoxides were synthesised for their value as pivotal building blocks for follow-up reactions. Notably, their ring opening with an amine can lead to amino alcohols. In our case, (pseudo)ephedrine was obtained, which is a valuable pharmaceutical drug.

E-factor comparison of the different biocatalytic systems studied

Table 6.1. Comparison of the systems presented in this thesis

	Max product formation (mM)	Enzymatic reaction challenge overcome	Limitations	E factor ^a
Chapter 2: HLADH/FMN/light ^b	9	Low cofactor concentration	Acidification of the reaction due to hydrolysis of lactones	885
Chapter 3: OYE/FMN/light ^c	36	No need of cofactors	Inactivation of enzyme overtime by light	259
Chapter 4: OYE/FMN/Cr ^d	10	No need of cofactors	High excess of metal needed	1434
Chapter 5: UPO in organic solvent ^e	360	High enzyme robustness toward organic solvent due to immobilisation	Poor enzyme recovery	31

^a The E factor is the weight of all the wastes (water, salt, chemical reagents and remaining substrate) divided by the weight of the actually formed product.

^b Conditions: 100 mM glycine-NaOH buffer pH 9 100 mM, [diol]₀ = 10 mM, [NADH]₀ = 1 mM, [FMN] = 100 μM, [HLADH] = 7.4 μM

^c Conditions: 100 mM potassium phosphate buffer (pH 6.5), [2-methylcyclohex-2-en-1-one] = 50 mM; [FMN] = 0.2 mM, [YqjM] = 6.9 μM, [EDTA] = 50 mM

^d Conditions: [purified YqjM] = 6.9 μM, [FMN] = 500 μM in KPi buffer 100 mM pH 6.5, [2-methylcyclohex-2-en-1-one] = 10 mM, 625 g/L of chromium powder <45 μm, 21 °C

^e Conditions: 10 mL *cis*-β-methylstyrene, [rAaeUPO@IB-COV-1]_{total} = 41.8 μM

Table 6.1 gives a comparison of the systems presented in this thesis based on product formation, challenges overcome, limitations and the E factor. The E factor is the weight of all the wastes divided by the weight of the actually formed product. The E-factor values of the different systems therefore results in a ranking in terms of environmental sustainability. It is seen in Table 6.1 that there is a correlation between the product concentration and the E factor. The system with the highest product formation (Chapter 5, peroxygenase in organic solvent), is characterised by an E factor as low as 31. The other extreme is Chapter 4 with an E factor of 1434. In this case, OYE is directly regenerated by chromium. Because this is not a catalytic system and stoichiometric amounts of metal are required, a lot of (heavy) chromium waste is produced. In all these systems, water – used as solvent – is classified as waste after the reaction. When comparing the use of OYE in chapters

3 and 4, the photoregeneration of OYE in chapter 3 is better in an environmental point of view, even though the enzymes are rapidly inactivated.

The system of Chapter 2 seems to be a green alternative due to the regeneration of cofactors by light. But its low product concentration – and consequently high amounts of waste water, in the end is not very environmentally friendly. A higher product concentration is thus required.

From these four systems, the epoxidation in neat organic solvent in Chapter 5 seems to be the best one. The advantage of using organic solvents lies in the simplification of the downstream and purification processes. A simple distillation step enables the recovery of the solvent while water treatment is more complex. According to Sheldon and the E factor,¹² this system is classified as reasonable due to its value (31), without obligatory consequent improvements, when compared to systems in pharmaceutical industry. It is good to note that in all these systems, the E factor of the enzyme production was not included. In reality this will lead to even higher values. The range of required productivity from Woodley¹³ also confirmed this comparison.

Additional comments and recommendations

In conclusion, it is clear that all systems have significant potential for synthetic application. However, we are not there yet. Below detailed suggestions are made for further studies for every individual system.

Chapter 2

In this chapter, increasing the substrate load caused an acidification of the reaction due to the hydrolysis of the lactone. To minimise or prevent this side reaction, controlling the pH with a pH-stat and extracting *in situ* the lactone would greatly improve the system.

The limitations of this system that should also be mentioned are the slow oxygen transfer rate and the light penetration. We aimed to increase the oxygen concentration in the reaction with O₂-filled balloons, but increasing the surface

between the liquid and the gas phases or working under higher pressure would definitively improve the oxygen concentration in the reaction. The system used will also need to be improved for its quantum efficiency. As the light is coming from outside the reaction, photons have to penetrate several layers of glassware and liquid to reach the reaction. A direct light illumination, i.e. light coming from inside the reaction is the solution of this limitation. With these recommendations, it should be possible to reach higher product concentrations.

Chapter 3

In the study of the enzyme's inactivation by light, we analysed by MS the flavoprotein after light illumination. We discovered that some methionine amino acids were oxidised. This later discovery suggests the presence of reactive oxygen species (ROS), probably because the system was not strictly anaerobic. In fact, photoexcited flavin will react with molecular oxygen and form the so-called ROS, hydrogen peroxide, hydroxyl radicals and singlet oxygen. The anaerobic conditions were chosen to avoid loss of reactivity due to this side reaction with oxygen. We degassed our reaction with N₂ to remove oxygen and kept a slight overpressure with N₂-filled balloons. However, we believe that this procedure was not sufficient, and still residual oxygen was left. Performing the reaction in a glovebox will probably lead to lesser deactivation of the flavoprotein. Another solution to improve this system for larger scale application is to develop a setup in which the enzyme is separated from the light source.

Finally, this study demonstrated that also flavin-independent enzymes such as formate dehydrogenase from *Candida boidinii* are light sensitive. The reason thereof is not clear, and needs to be further investigated. With these results in mind, we became more careful with light, even with sunlight, while handling enzymes.

Chapter 4

The system of chapter 4 is a funky proof-of-concept of the metalloregeneration of Old Yellow Enzymes. The principle is interesting from a scientific point of view but

Chapter 6

so far not viable for large scale application. High excess of chromium is needed for the reaction to reach full conversion due to the natural oxidation of the surface of the metal by oxygen. As metals are becoming a rare element, they are also expensive and need to be recycled after the reaction. More research will be needed to improve the economic aspects of this system, such as using nanoparticles to enable higher surface interaction. The reduction of the flavoprotein by zinc, although not very selective, can be explored further by using a two-liquid phases system where the zinc can be separated from the substrate and product for avoiding most of the chemical reduction.

Chapter 5

Peroxides are cosubstrates of peroxygenases. They are cheaper than nicotinamide and flavin cofactors, but have the disadvantage to be toxic to enzymes. In our neat organic solvent study, we fed the reaction system overtime with organic peroxides to avoid inactivation of enzymes. However, this addition of peroxides can still generate hot spots in the reaction which cause denaturation of the enzymes. That is why, for future prospects, *in situ* generation of organic peroxide is highly desirable. So far though, we are unaware of possibilities that are compatible with an enzymatic reaction. A second advantage of this *in situ* generation is that the working volume would stay constant and therefore no further dilution of our product occurs.

In this system, the enzyme's immobilisation should also be improved. The low catalytic activity remaining after immobilisation and therewith the impossibility to regenerate the enzyme, are important drawbacks.

As overall conclusion we want to state that, compared with chemical reactions, the substrate loading remains low in biocatalysis. Simply showing high conversions in a biocatalytic reaction is not enough. For future studies more attention needs to be paid to reach higher substrate loadings.

As to photobiocatalysis a main observation is that enzymes can be quite vulnerable to the light. A recent interesting study by the group of Hyster¹⁴ showed that

photochemistry with enzymes could be used to create radicals, leading to new reactions. This is a noteworthy development that could well lead the way for photochemistry in biocatalysis.

References

1. C.E. Paul, I. Lavandera, V. Gotor-Fernández, W. Kroutil, V. Gotor, *ChemCatChem* 2013, **5**, 3875–3881.
2. T. Orbeagozo, I. Lavandera, W.M.F. Fabian, B. Mautner, J.G. de Vries, W. Kroutil, *Tetrahedron*, 2009, **65**, 6805-6809.
3. I. Lavandera, A. Kern, V. Resch, B. Ferreira-Silva, A. Glieder, W.M.F. Fabian, S. de Wildeman, W. Kroutil, *Org. Lett.*, 2008, **10**, 2155-2158.
4. W. Kroutil, H. Mang, K. Edegger, K. Faber, *Adv. Synth. Catal.*, 2004, **346**, 125-142.
5. J.T. Park, J.-I. Hirano, V. Thangavel, B.R. Riebel, A.S. Bommarius. *J. Mol. Catal. B: Enzym.*, 2011, **71**, 159-165.
6. R. Jiang, A.S. Bommarius. *Tetrahedron Asymm.*, 2004, **15**, 2939-2944.
7. B.R. Riebel, P.R. Gibbs, W.B. Wellborn, A.S. Bommarius, *Adv. Synth. Catal.*, 2003, **345**, 707-712.
8. B.R. Riebel, P.R. Gibbs, W.B. Wellborn, A.S. Bommarius, *Adv. Synth. Catal.*, 2002, **344**, 1156-1168.
9. M. Mifsud Grau, J.C. van der Toorn, L.G. Otten, P. Macheroux, A. Taglieber, F.E. Zilly, I.W.C.E. Arends, F. Hollmann, *Adv. Synth. Catal.*, 2009, **351**, 3279-3286.
10. J.S. Dordick, M. A. Marletta, A. M. Klivanov, *Proc. Natl. Acad. Sci. U. S. A.*, 1986, **83**, 6255-6257
11. A. Zaks, A. M. Klivanov, *Science*, 1984, **224**, 1249-1251.
12. R.A. Sheldon, *Chem. Commun.*, 2008, **29**, 3352-3365.
13. P. Tufvesson, J. Lima-Ramos, M. Nordblad, J.M. Woodley, *Org. Process Res. Dev.*, 2011, **15**, 266-274.
14. M.A. Emmanuel, N.R. Greenberg, D. G. Oblinsky, T. K. Hyster, *Nature*, 2016, **540**, 414.

Curriculum vitae
and
List of publications

Curriculum vitae



Marine Charlène Renée Rauch was born in Sarreguemines, France the 7th of June 1991 where she grew up. After her Baccalauréat, she moved to Strasbourg to undertake a three-year intensive course in Lycée Kléber preparing for the competitive exam required to enter a “Grande École”. She succeeded and entered the Chemical Engineering School of Mulhouse (ENSCMu) where she studied chemistry for three years. During the second year, she discovered the beauty of biocatalysis and decided to specialise in organic, bioorganic and pharmaceutical chemistry. She performed during the third year an internship at Novartis Institutes for BioMedical Research in Basel, Switzerland in the Bioreactions group of the Global Discovery Chemistry department, led at the time by Dr. Stefan Lütz. She worked on the optimisation of prenyl transferases activity. In October 2015, she started her PhD study in the group of Prof. Dr. Frank Hollmann in Delft, The Netherlands working with different enzymes such as Old Yellow Enzymes and peroxygenases.

List of publications

M.C.R. Rauch, Y. Gallou, L. Delorme, C.E. Paul, I.W.C.E. Arends, F. Hollmann, Metals in biotechnology: Cr-driven-stereoselective reduction of conjugated C=C-double bonds, *ChemBioChem*, 2019, **20**, 1-5.

M.C.R. Rauch, M. Pesic, M.M.E. Huijbers, M. Pabst, C.E. Paul, I.W.C.E. Arends, F. Hollmann, Photochemical regeneration of flavoenzymes – an Old Yellow Enzyme case-study; *BBA – Proteins Proteomics*, 2020, **1868**, 140303.

M.C.R. Rauch, F. Tieves, C.E. Paul, I.W.C.E. Arends, M. Alcalde, F. Hollmann; Peroxygenase-catalysed epoxidation of styrene derivatives in neat reaction media; *ChemCatChem*, 2019, **11**, 4519-4523.

Y. Ma, Y. Li, S. Ali, P. Li, W. Zhang, M.C.R. Rauch, S. J.-P. Willot, D. Ribitsch, Y.H. Choi, M. Alcalde, F. Hollmann, Y. Wang; Natural deep eutectic solvents as performance additives for Peroxygenase catalysis; *ChemCatChem*, 2019, **11**, 1-7.

F. Tieves, S.J.-P. Willot, M.M.C.H. van Schie, M.C.R. Rauch, S.H.H. Younes, W. Zhang, J. Dong, P. Gomez de Santos, J.M. Robbins, B. Bommarius, M. Alcalde, A.S. Bommarius, F. Hollmann; Formate Oxidase (FOx) from *Aspergillus oryzae*: one catalyst enables diverse H₂O₂-dependent biocatalytic oxidation reactions; *Angew. Chem. Int. Ed.*, 2019, **58**, 7873-7877.

J. Yoon, S.H. Lee, F. Tieves, M.C.R. Rauch, F. Hollmann, C.B. Park; Light-harvesting dye-alginate hydrogel for solar-driven, sustainable biocatalysis of asymmetric hydrogenation; *ACS Sustain. Chem. Eng.*, 2019, **7**, 5632-5637.

M.M.C.H. van Schie, S.H.H. Younes, M.C.R. Rauch, M. Pesic, C.E. Paul, I.W.C.E. Arends, F. Hollmann; Deazaflavins as photocatalysts for the direct reductive regeneration of flavoenzymes; *Mol. Catal.*, 2018, **452**, 277-283.

M.C.R. Rauch, S. Schmidt, I.W.C.E. Arends, K. Oppelt, S. Kara, F. Hollmann; Photobiocatalytic alcohol oxidation using LED light sources; *Green Chem.*, 2017, **19**, 376-379.

Acknowledgements

It is with a great joy that I finally finished my PhD. These four years have been a great experience from a scientific point of view but also for my personal development. Delft is a lovely Dutch city where I met so many people. I really liked to work in this multidisciplinary and multicultural environment. Without you all, I would not have managed these four years and I want to thank you all for that.

First I would like to thank my promotor Frank Hollmann for the PhD opportunity. You allowed me to work on these projects with a huge freedom. You were always making sure that we were not missing lab equipment, and you sent us to so many nice conferences over the world. That was great! It was not always easy, but with all your overflowing ideas, I learned to prioritise the work I had to do. Thank you also for the nice team we had, I learned a lot with them in a delightful atmosphere. It has been also really nice from you to trust Sébastien and me; I can imagine that it had been a difficult choice to hire him.

Then I would like to thank Isabel Arends, my second promotor, for the help during my PhD. I think you understood me, in my way of working and being. You were an important support. Your smile and joy have been always welcome. Thank you for the time you take for helping me, especially during the writing process.

Caroline, je sais que ces mots-là ne suffiront pas pour te montrer ma gratitude. De ton Post-doc à encore maintenant, tu as toujours été présente et disponible pour moi. C'est toi qui m'as appris toutes les ficelles de la biocatalyse quand je suis arrivée dans le groupe et je ne pourrais jamais te remercier assez. En devenant ma copromoteur, tu t'es encore plus impliquée dans mes projets et ça a été pour moi une vrai bouffée d'oxygène. Nos longues conversations scientifiques et personnelles, le tennis, nos séances de zumba, tes mots de motivation, les soirées et dîners presque improvisés vont me manquer. Je te remercie du fond du cœur d'être toi.

A special thanks to Mieke van der Kooij; you are a great person with talented organisation skills. Without you the group would be quite lost.

Let's talk about my squad now: Morten, Georg and Seb. These few words won't be enough to express my feelings and appreciation. But, thank you very much for these four amazing years we had together as a team. We had a lot of fun in the lab but also during conferences, dinner, week-end and even during holidays. Without you, these four years would have been boring and I am really grateful. I couldn't dream for better partners! Thanks a lot for your support!!

Special thanks to my Tally (Hanna): we started this PhD together and we finished it together. And in the path of it, we always supported each other in the good and in the bad moment. I miss our language-cocktails sessions. I wish you all the best in Hamburg! XOXO

All this work would not have been possible with the great team of researcher that always had my back: Tiago, thanks for helping me with the electrochemistry and all the nice time we had together, keep your smile forever! ; Sandy, Mieke and Florian, thanks for your help in the MB lab and for teaching me some biochemistry knowledge I was missing; Andrada, thank you very much for your emotional support during this last year, I really appreciated it.

Thanks to the guests who came and freshened up the social events: Carmen, Pati (thank you for introducing us to Gloomhaven!), Gonzalo, amongst others...

I am very much thankful to all the technicians from the group: Maarten Gorseling for your energy in the lab and all your help, even if you left us for a more rainy country; Remco for keeping all the GC in a good state and for the extras discussions in our office; Marc for all your bad jokes (we still like you!) and for all the advices during my PhD; Laura for all your knowledge in the MB lab, I didn't use it so much, but when I needed help, you were always present! Lloyd, thanks for all the nice discussions at lunch and taking over the lab cleaning organisation, hope to meet you soon at a next concert! Stephen for all the nice pictures you always take (Thanks for being my official photographer!) and for taking care of the NMR.

Dank jullie wel

During these four years, I had the chance to supervise four students: Nicole, Léna, Lucas and Yann. Thank you very much for your hard work. I had a lot of fun and pleasure to guide you during your stay. I loved the time we had together. Thanks!

I want to express my deep sense of gratitude to all BOC members. Thank you for the great atmosphere we had, I couldn't hope better colleagues. Nati, thank you for being there and motivating me to be less lazy! Thanks to Caro, Fabio, Eman, Tania, for the great time we had together. Good luck to those who still have to finish their PhD, Luuk, Stefan, Albert, José, Retna, Alexandra, Sam, Xiaomin but don't forget to have fun! Jonathan, thanks for your craziness and all the good moment but also those where I could have killed you! Ashmiani, thanks for all the hugs and you happiness! Linda for your devotion to help us, always with a smile, and keep smiling! Thank you to all the staff of BOC, Ulf, Fred, Kristina, Peter-Leon, Duncan, without you, BOC would not be exceptional.

Je voudrais spécialement remercier mes amis que je vais retrouver en France. Les soirées jeux de société, jeux-vidéo, les nouvel ans, partir en vacances dans les montagnes, etc qu'on s'est organisés ces quatre dernières années m'ont vraiment fait du bien. Merci d'être là !

Aussi, que ferions-nous sans sa famille ? En étant séparé de ma famille par un pays, j'ai pris conscience du besoin que j'avais d'être près d'eux. Les vacances passées avec eux (aux Pays-Bas, en Lorraine, Alsace, sud de la France, Disneyland, Italie, ...) me redonnaient l'énergie nécessaire pour continuer et terminer ce doctorat. Tant de choses se sont passées durant ces quatre années, auxquelles je n'ai pas pu être présente comme je l'aurai souhaité. Merci à ma grand-mère, mes parents, mes beaux-parents, ma sœur, mes beaux-frères, mes belles-sœurs, mes cousins, mes tantes et oncles, mes neveux et nièces, mes filleuls (actuels et celui ou celle qui reste encore bien au chaud). Vous me remplissez tellement d'amour !

Je vous aime <3

Un grand merci à ma sœur, Delphine, qui a conçu cette belle couverture de thèse avec l'aide de ma cousine Anne. Merci à vous deux d'être présentes dans ma vie !

Finalement, je voudrais remercier l'homme de ma vie : Seb. Celui qui a choisi de me suivre dans cette aventure à l'étranger et de faire sa thèse avec moi, dans le même bureau, à côté de ma paillasse, dans un domaine qu'il ne pensait pas un jour travailler. Être 24h/24, 7j/7 ensemble n'a pas fragilisé notre lien, au contraire on en ressort plus fort. Merci d'être toujours là pour moi, dans les bons comme dans les mauvais moments, d'être un support constant et de me donner ton amour. Je t'aime plus que tout au monde.

